Sudan University of Science and Technology

College of Graduate Studies

Evaluation of the Sensitivity of Poly Vinyl Alcohol Films Doped with Silver Nitrate to Low X-ray Doses

تقييم حساسية أفلام البولي فينايل الكحول المطعمة بنترات الفضة للأشعة السينية المنخفضة

A thesis submitted for the fulfillment of the award of PhD in Physics

By:

Abdalla Mohamed Eldoma Mohamed

Supervisor:

Prof. Nadia Omar Al-Atta

Co-supervisor

Dr. Ahmed Elhassan Elfaki

November 2019

الآيـــــــــة

قـــــــــال تعالى :

﴿ اللَّهُ نُورُ السَّمَاوَاتِ وَالْأَرْضِ مَثَلُ نُورِهِ كَمِشْكَاةٍ فِيهَا مِصْبَاحٌ الْمِصْبَاحُ فِي زُجَاجَةٍ الزُّجَاجَةُ كَأَنَّهَا كَوْكَبٌ دُرِّيٌّ يُوقَدُ مِنْ شَجَرَةٍ مُبَارَكَةٍ زَيْتُونَةٍ لَا شَرْقِيَّةٍ وَلَا غَرْبِيَّةٍ يَكَادُ زَيْتُهَا يُضِيءُ وَلَوْ لَمْ تَمْسَسْهُ نَارٌ نُورٌ عَلَى نُورٍ يَهْدِي اللَّهُ لِنُورِهِ مَنْ يَشَاءُ وَيَضْرِبُ اللَّهُ الْأَمْثَالَ لِلنَّاسِ وَاللَّهُ بِكُلِّ شَيْءٍ عَلِيمٌ ﴾

سورة النور الاية ﴿35﴾

﴿وَيَسْئَلُونَكَ عَنِ الرُّوحِ قُلِ الرُّوحُ مِنْ أَمْرِ رَبِّي وَما أُوتِيتُمْ مِنَ الْعِلْمِ إِلاَّ قَلِيلًا﴾

سورة الإسراء الاية ﴿85﴾

Dedication

Every challenging work needs self-efforts as well as guidance of elders especially those whom were very close to our heart.

To those of the fingers to give us a life of happiness.

My humble effort I dedicate to my sweet and lovely mother.

To reap the thorns out of my way for me to pave the way science

To heart the great my father

I ask Allah to mercy my dear father and forgive you and shed your soul paradise

Along with all hard working and respected teachers

To my brothers, sisters, friends, and to all my family.

Acknowledgements

First and foremost, I would like to express my deepest gratitude to

Prof. Nadia Omer alatta, Special Thanks to Dr. Ahmed hassan

Alfaki without their helps this work could not have been

accomplished

My thanks also go to Medical Modern Center, Alneelain University,

National Cancer Institute – Algazira University, X-ray Lab at

SSMo – planning and research unit at SSMo.

Deep thanks to my family for their consistent support.

Finally, special thanks to my brother Khalid Yagoup for his

great support to me, and I wish him more success and

excellence.

Abstract

This research pertains to study the sensitivity of Poly Vinyl Alcohol Films Doped with Silver Nitrate to Low X-ray Doses and their uses as chemical Radiation Dosimeter, Studied on irradiated polymers show many advantages of induced radiation changes on which can be quantified and qualitied to deduce the amount of radiation dose and exposure in diagnostic radiology, The PVA/$AgNO_3$ Films were made through solvent casting technique with seven concentrations of $AgNO_3$/PVA percentage and that is (C_1, C_2, C_3, C_4, C_5, C_6, C_7), by dissolving each concentration of PVA powder in 100 ml distilled water at room temperature on a beaker and The solutions were magnetically stirred at room temperature for 3 hours and then the PVA/$AgNO_3$ solutions poured in a petri-dish to form films by casting method in dark room. and left to dry at ambient temperature at least 2 days. Then films were peeled off in the petri-dish, cut into small films 2x2cm, loaded in sealed dark dental film envelope, then the PVA/$AgNO_3$ films were irradiated with low x-ray doses in the range of diagnostic levels, [.15, 33, .59, .93, 1.34] mGy and The sensitivity of PVA/$AgNO_3$ films were characterized using optical densitometer and UV-vis spectrophotometer, the result showed that the irradiation of the PVA\$AgNo_3$ films with x-ray doses induces color change and The color intensity was increase with increasing x-ray doses, the optical densitometer analysis showed positive correlation between $AgNO_3$ concentrations and optical density of PVA/$AgNO_3$ and positive correlation between x-ray doses and optical density of PVA/$AgNO_3$, the UV-vis spectrophotometer analysis of PVA/$AgNO_3$ films showed absorption peak at the wavelengths [430, 435, 434, 445, 442] nm for films prepared with (4) wt% of $AgNO_3$ irradiated with x-ray doses [0.15, 0.33, 0.59, 0.93, 1.34] mGy, and the intensity of peaks is proportional to the x-ray dose, in addition to the specific absorbance and absorption coefficient is directly proportional to the irradiated x-ray doses, the conclusion the synthetic PVA/ $AgNO_3$ films showed good response to low x-ray doses it can be used as chemical radiation dosimeters in diagnostic radiology centers.

ملخص البحث

يهدف هذا البحث لدراسة حساسية أفلام البولي فينايل الكحول المطعمة بالفضة للأشعة السينية المنخفضة وإستخدامها كمقياس كيميائي للأشعة وقد أظهرت الدراسة على البوليمرات المشعة العديد من مزايا التغيرات الإشعاعية المستحثة والتي يمكن قياسها كميا ونوعيا لايجاد مقدار الجرعة الإشعاعية والتعرض في الأشعة التشخيصية، تم تصنيع أفلام [PVA/AgNO3]من خلال تقنية المذيبات بسبعة تراكيزمن نترات الفضة [AgNO3] ,[C2=5%], [C1=4%] [C3=6%], [C4=10%], [C5=15%], [C6=20%], [C7=25%] عن طريق إذابة كل تركيز من مسحوق البولي فينايل الكحول [PVA/ AgNO3] في [100] مل من الماء المقطر في درجة حرارة الغرفة على دورق وتم تحريك المحلول مغناطيسياً في درجة حرارة الغرفة لمدة 3 ساعات ثم سكبت محاليل [PVA / AgNO3] في طبق زجاجي لتشكيل الأفلام بواسطة طريقة تقنية المذيبات في غرفة مظلمة .وتم تجفيف الأفلام في درجة حرارة الغرفة لمدة يومين على الأقل ثم وضعت الأفلام في ظرف بلاستيكي مظلم لحمايتها من الضوء. ثم تم تشعيع أفلام [$PVA/AgNO_3$] بجرعات منخفضة من الأشعة السينية في حدود مستويات الأشعة التشخيص [.15,.33,.59,.93,1.34] ملي قري وقد أظهرت الدراسة تغير في لون الأفلام وتزيد شدة اللون بزيادة بزيادة الجرعة الأشعة السينية وتمت دراسة خصائص أفلام [$PVA/AgNO_3$] بعد التشعيع بواسطة مطياف الأشعة فوق البنفسجية والمرئية ومقياس الكثافة الضوئية،أظهرت نتائج تحليل الكثافة الضوئية وجود علاقة خطية بين الكثافة الضوئية للفلم وتركيز [PVA/ AgNO3] وكذلك علاقة خطية بين الكثافة الضوئية للفلم وجرعة الأشعة السينية المطبقة ، وأظهرت نتائج تحليل مطياف الأشعة فوق البنفسجية والمرئية لأفلام [$PVA/AgNO_3$] المصنعة بتركيز [4%wt] والمعرضة لجرعات أشعة سينية mGy [.15, .33, .59, .93, 1.34] طيف امتصاص عند الأطوال الموجية [430,435,434,445, 442] نانومتر وتتناسب شدة طيف الإمتصاص طرديا مع شدة جرعة الأشعة السينية المطبقة بالإضافة إلى ذلك معامل الامتصاص والامتصاص المحدد يتناسبان طرديا مع جرعات الأشعة السينية المطبقة ، وخلاصة الدراسة أن أفلام [$PVA/AgNO_3$] المصنعة أظهرت استجابة جيدة لجرعات الأشعة السينية المنخفضة ، ويمكن استخدامها كمقاييس كيميائي لجرعات الأشعة السينية في مراكز الأشعة التشخيصية.

Contents

List of Tables

List of figures

Abbreviations

Abbreviation	statement
PVA	Polyvinyl alcohol
$AgNO_3$	Silver Nitrate
TLD	Thermos luminescent dosimeter
KeV	Kilo electron volt
mGy	mili Gray
KVp	Kilo voltage peak
mAs	Mili ampere second
FSD	Focal to skin distance
MeV	Mega electron volt
CR	Computed radiography
IAEA	International atomic energy agency
ESAK	Entrance surface air kerma
ESD	entrance skin dose
NRPB	National Radiation Protection Board
OSL	optically stimulated luminescence
BSF	backscatter factor.

Chapter one: Introduction

Introduction:

Dosimetry plays an important role in the quality control of radiation processing (W. L. McLaughlin, et al, 1989). Now a day's radio chromic film dosimeters are used widely for radiation dosimetry of different types (M. Kattan, Y, et al, 2006). Many film dosimeters are used for radiation dosimetry such as radio chromic plastic films of various types and some polymers (M. Kattan Y, et al, 1989) PVA films are easy to prepare and used for routine irradiation processes of food and medical equipment's (N. V. Bhat, et al, 2007). For daily dose monitoring in radiation processing, the polymeric poly vinyl Alcohol dyed flexible films are considered to be the most common ones as dosimeters (A. Miller, 1986). because of their exceptional chemical and physical properties [(Lee, H, et al, 2011), (Han, D, et al, 2011)], biocompatibility, stability to temperature variation, and non-toxicity [(Mutsuo, S., et al, 2011), (Shuai, C, et al, 2013)]. PVA has fascinating properties and a wide variety of applications. Also, it has high dielectric strength, good charge storage capacity, high elasticity and good film forming by solution casting (Li W, et al, 2013). Exposure of polymer materials to ionizing radiation produces changes in the microstructural properties, which affects the optical, the polymer materials (Arshak, K, et al, 2003). Dye dosimetry is based on the fact that ionizing radiations interact with matter and

cause the color change of the dye. This property of color change of dye can be used for dosimetry as the decomposition of dye is linear with respect to the amount of dose absorbed [(Parwate DV, et al, 2007), (Al-Zahrany AA, et al, 2011), (Blaskov V, et al, 2011), (Chen YP, et al, 2008)]. The high energy ionizing radiations bring the radiolysis of the dye (de coloration or bleaching effect) which is used to measure the energy of the radiation incident on the chemical system [(Patel HM, et al, 2012), (Khanmohammadi H, et al, 2012)]. All metallic nanoparticles (Gold, Silver, Platinum…etc) exhibit unusual electrical, magnetic, optical and electrochemical properties due the near-free conduction electrons, which are depend on their size, surface Plasmon, surface free energy and surface area, as well as on the surrounding dielectrics, The polymer/silver nanocomposites revealed that the prosperities of silver within it is composites answer many potential applications in optical waveguides, optical switches, molecular identification, oxidative catalysis, antimicrobial effects, etc. These mentioned properties are `dependent on the particle size, shapes and the method of composites synthesis. Varieties of synthesis method have been developed, including reduction from metallic salts, ultrasonic irradiation technique, ion implantation, and thermal process and microwave technique (Stakheev A.Y, et al, 1999). The radiation measurements in this study will be depend on the optical density measurement and optical absorbance measurement using optical densitometer and UV-visible spectroscopy accordingly. The expected x-ray exposure on the

silver/PVA composites film will be as color change to yellow or golden due to presence of silver while the expected change on PVA will be as degradation of the PVA chain (Ali Z.I., et al, 2006).

1.2. Problem of Statement:

Lacking the frequent radiation exposure assessment tools, hence it will be as a fast, easy and cheap assessment tool with a presence of densitometer which is the cheapest equipment used in the radiation exposure assessment. the following study will help to establish a local in vivo dosimeter system to monitor radiation dose with local available materials in diagnostic centers.

1.3. Significant of the study:

Ionizing radiation has significant capabilities to induce chemical and physical change in the exposed materials. Studied on irradiated polymers show many advantage of induced radiation changes on which can be quantify and qualify to deduce the amount of radiation dose and exposure. This method relative to other methods such as film badge is so simple and easy. The advantage includes no developer, no fixer, no other effecting factors, the process occurred at a solid-site condition, fast method and inexpensive, environmental friendly and controllable acquisition.

1.4. Objectives of the study:

1.4.1. General Objective:

To study the Sensitivity of Poly Vinyl Alcohol Films Doped with Silver Nitrate to Low X-ray Doses.

1.4.2. Specific Objectives:

- To explore the synthetic of PVA/$AgNO_3$ films to be used as chemical radiation dosimeters.
- To evaluate and asses the sensitivity of PVA/$AgNO_3$ composites films to low x-ray doses.
- To measure the absorption spectra post irradiation.
- Evaluate and assess the effect of $AgNO_3$ concentrations in the PVA/$AgNO_3$ composites films.
- To measure the Specific Absorbance of the PVA/$AgNO_3$ composites films.
- To measure the absorption coefficient of the PVA/$AgNO_3$ composites films.
- To compare the PVA/$AgNO_3$ composites film exposure data with TLD.
- To find the correlation between the Optical Density and applied radiation dose.
- To find the correlation between the Optical Density and PVA/$AgNO_3$ concentrations.
- To find the correlation between the Specific Absorbance and applied radiation dose.
- To find the correlation between the absorption coefficient and applied radiation dose.

1.5. Thesis Layout:

The structure of the thesis will be formed of five chapters. Chapter one will deal with the general introduction about the research background, problem statement, Significant of the study and the objectives of the study. Chapter two will deal with literatures review cover the theoretical background and previous studies. Chapter three will deal with the methodology of the study, Chapter four will cover the results. And chapter five will cover discussion, conclusion, recommendations, references.

Chapter two

Theoretical Background and literature Review

2.1. Ionizing Radiation:

Ionizing (high-energy) radiation has the ability to remove electrons from atoms; i.e., to ionize the atoms (Murat, 2010). Ionizing radiation can ionize matter, either directly or indirectly:

2.1.1. Directly ionizing radiation: Fast charged particles that deposit their energy in matter directly, through many small Coulomb (electrostatic) interactions with orbital electrons along the particle track (D.R. Dance et al, 2014).

2.1.2. Indirectly ionizing radiation: X or gamma ray photons or neutrons that first transfer their energy to fast charged particles released in one or a few interactions in the matter through which they pass. The resulting fast charged particles then deposit their energy directly in the matter (D.R. Dance et al, 2014). Ionizing radiation can be electromagnetic or particulate radiation as shown in the (Figure. 2.1). (Murat, 2010).

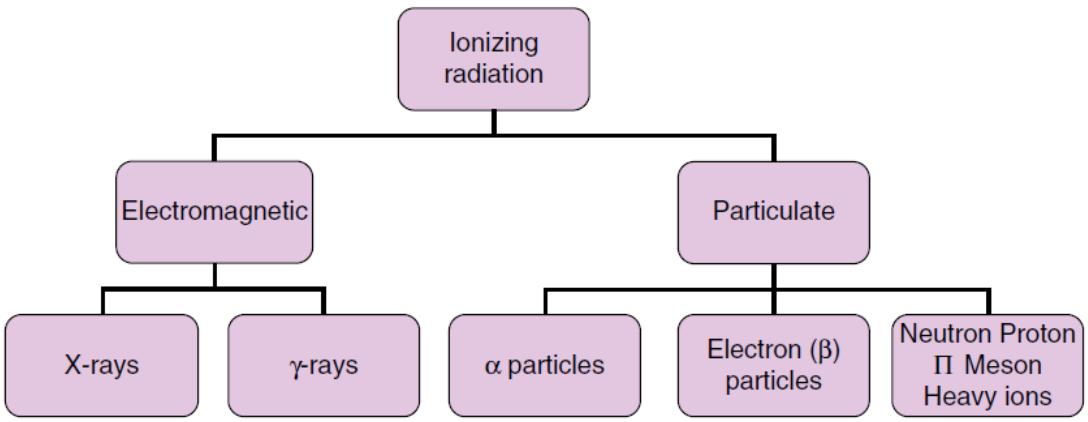

Figure (2.1) shows the types of Ionizing radiation (Murat, 2010).

2.2. X-Rays:

X-rays were discovered by Roentgen in 1895 when high-speed electrons are decelerated on collision with high atomic number material while studying cathode rays (stream of electrons) in a gas discharge tube. He observed that another type of radiation was produced (presumably by the interaction of electrons with the glass walls of the tube) that could be detected outside the tube. This radiation could penetrate opaque substances, produce fluorescence, blacken a photographic plate, and ionize a gas. He named the new radiation x-rays (ICRP, 2001).

2.2.1. Production of X-Rays:

X-rays are produced by two different effects:

1. By decelerating energetic electrons (ranging from keV to MeV) bremsstrahlung is produced with a continuous spectral intensity distribution I(λ), which depends on the energy of the electrons.

2. The energetic electrons can excite inner shell transitions in the atoms of the anode. The excited states Ei emit X-rays as spectral lines on transitions Ei → Ek with wavelengths λik, characteristic for the anode material. These X-rays are therefore called characteristic X-ray radiation (Wolfgang Demtroder, 2006).

2.2.1.1. Bremsstrahlung X-rays:

The process of bremsstrahlung is the result of radiative interaction between a high-speed electron and a nucleus. The electron while passing near a nucleus

may be deflected from in path by the action of Coulomb forces of attraction and loses energy as bremsstrahlung, a phenomenon predicted by Maxwell's general theory of electromagnetic radiation. According to this theory, energy is propagated through space by electromagnetic fields. As the electron, with its associated electromagnetic field, passes in the vicinity of a nucleus; it suffers a sudden deflection and acceleration. As a result, a part or all of its energy is dissociated from it and propagates in space as electromagnetic radiation. Since an electron may have one or more bremsstrahlung interactions in the material and an interaction may result in partial or complete loss of electron energy, the resulting bremsstrahlung photon may have any energy up to the initial energy of the electron. Also, the direction of emission of bremsstrahlung photons depends on the energy of the incident electrons. At electron energies below about 100 KeV, X-rays are emitted more or less equally in all directions (Bushberg JT et al , 2002).

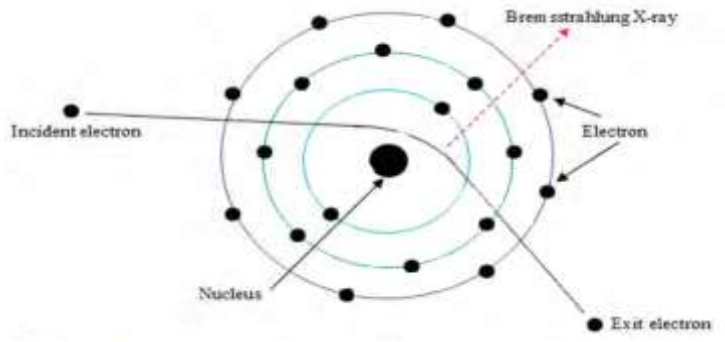

Figure (2.2) shows the Bremsstrahlung X-rays (Ronald Denderehand, 2014)

2.2.1.2. Characteristics X-rays:

Electrons incident on the target also produce characteristic X-rays. An electron with kinetic energy E_0, may interact with the atoms of the target by ejecting an orbital electron, such as a K, L, or M electron, leaving the atom ionized.The original electron will recede from the collision with energy when a vacancy is created in an orbit, an outer orbital electron will fall down to fill that vacancy. In doing so, the energy is radiated in the form of electromagnetic radiation. This is called characteristic radiation, i.e., characteristic of the atoms in the target and of the shells between which the transitions took place. With higher atomic number targets and the transitions involving inner shells such as K, L, M, and N, the characteristic radiations emitted are of high enough energies to be considered in the X-ray part of the electromagnetic spectrum (Bushberg JT et al , 2002).

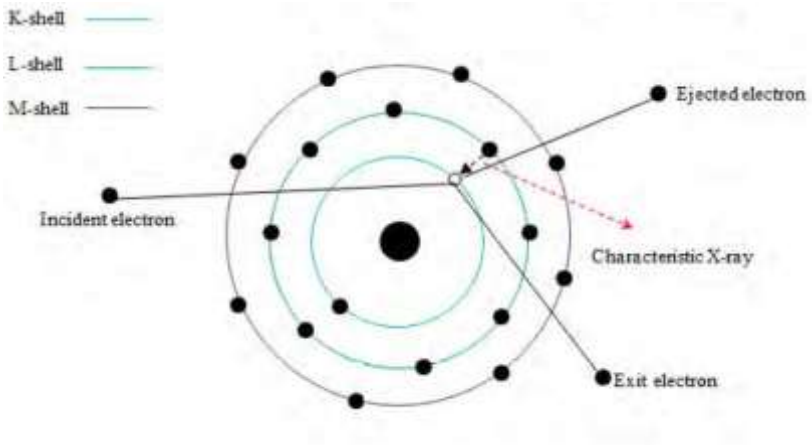

Figure (2.3) shows the Characteristics X-rays (Ronald Denderehand, 2014)

2.2.2. Spectrum of X-ray:

X-ray photons produced by an X-ray machine are heterogeneous in energy. The energy spectrum shows a continuous distribution of energies for the bremsstrahlung photons superimposed by characteristic radiation of discrete energies. A typical spectral distribution is shown in Fig. The inherent filtration in conventional X-ray tubes is usually equivalent to about 0.5- to 1.0-mm aluminum. Added filtration, placed externally to the tube, further modifies the spectrum. It should be noted that the filtration affects primarily the initial low-energy part of the spectrum and does not affect significantly the high energy photon distribution. The purpose of the added filtration is to enrich the beam with higher-energy photons by absorbing the lower energy components of the spectrum. As the filtration is increased, the transmitted beam hardens, i.e., it achieves higher average energy and therefore greater penetrating power. Thus the addition of filtration is one way of improving the penetrating power of the beam. The other method, of course, is by increasing the voltage across the tube. Since the total intensity of the beam (area under the curves in Fig. 2.4**)** decreases with increasing filtration and increases with voltage, a proper combination of voltage and filtration is required to achieve desired hardening of the beam as well as acceptable intensity. The shape of the X-ray energy spectrum is the result of the alternating voltage applied to the tube, multiple bremsstrahlung interactions within the target and filtration in the beam. However, even if the X-ray tube were to be energized with a

constant potential, the X-ray beam would still be heterogeneous in energy because of the multiple bremsstrahlung processes that result in different energy photons. Because of the X-ray beam having a spectral distribution of energies, which depends on voltage as well as filtration, it is difficult to characterize the beam quality in terms of energy, penetrating power, or degree of beam hardening. A rule of thumb is often used which states that the average X-ray energy is approximately one-third of the maximum energy or KVp. Of course, the one-third rule is a rough approximation since filtration significantly alters the average energy. Another quantity, known as half-value layer, has been defined to describe the quality of an X-ray beam (Bushberg JT et al , 2002).

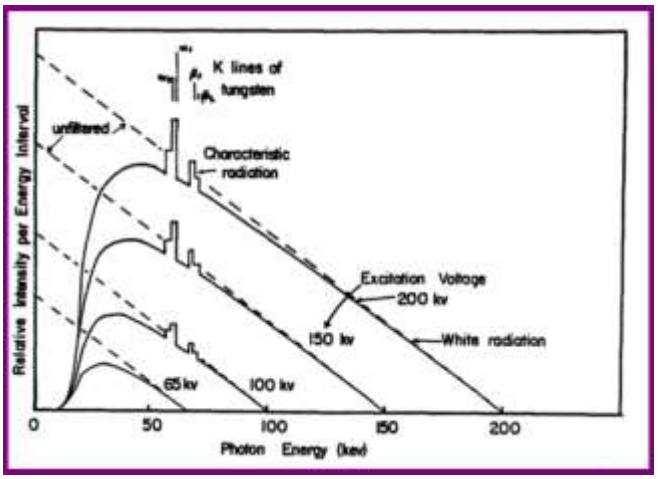

The figure (2.4) show the Spectral distributions of X-rays (Bushberg JT et al ,2002).

2.2.3. X-ray Tube:

Figure (2-5) shows the main components of a modern x-ray tube. A heated filament releases electrons that are accelerated across a high voltage onto a

target. The stream of accelerated electrons is referred to as the *tube current*. X rays are produced as the electrons interact in the target. The x rays emerge from the target in all directions but are restricted by collimators to form a useful beam of x rays. A vacuum is maintained inside the glass envelope of the x-ray tube to prevent the electrons from interacting with gas molecules. (William R. Hendee et al, 2002).

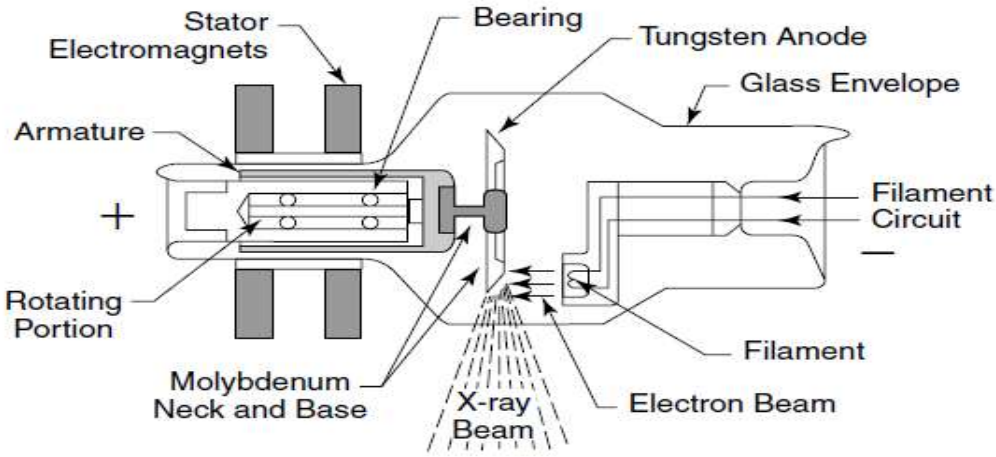

The figure (2.5) show the main component of X-ray tube (William R. Hendee et al, 2002)

2.2.4. Absorption of X-rays:

X-rays which enter a sample are scattered by electrons around the nucleus of atoms in the sample. The scattering usually occurs in various different directions other than the direction of the incident X-rays, even if photoelectric absorption does not occur. As a result, the reduction in intensity of X-rays which penetrate the substance is necessarily detected. When X-rays with intensity I0 penetrate a uniform substance, the intensity I after transmission through distance x is given by:

$$I = I_0 e^{-\mu x}$$

Here, the proportional factor _ is called linear absorption coefficient, which is dependent on the wavelength of X-rays, the physical state (gas, liquid, and solid) or density of the substance, and its unit is usually inverse of distance (Yoshio Waseda et al,2011).

2.2.5. Interaction of radiation with matter:

Ionizing radiation interacts with matter depending on its nature: directly ionizing radiation (charged particles) and indirectly ionizing radiation (uncharged particles). Charged particles interact with nearly every atom along its path, depositing their energy in the medium through direct Coulomb-force interactions with the nearby atoms and losing their energy gradually. These Coulomb-force interactions are characterized in terms of the relative sizes of the impact parameter and the atomic radius into soft and hard collision, and bremsstrahlung radiation (Andreo et al., 2017). Uncharged particles, by contrast, may pass through matter with no interactions at all.

They deposit their energy by a two-step process: first they transfer their energy to charged particles, and then these charged particles will deliver their energy to matter as previously mentioned (Glenn F. Knoll, 2010).

2.2.5.1. Interaction of photon with matter:

When traversing matter, photons will penetrate, scatter, or be absorbed. There are five major types of interactions of x- and gamma-ray photons with matter, the first three of which play arole in diagnostic radiology an: (a) Compton

scattering, (b) photoelectric absorption, and (c) pair production (Bushberg et al.,2002).

2.2.5.1.1. Compton scatters:

Compton scattering (also called inelastic or nonclassical scattering) is the predominant interaction of x-ray and gamma-ray photons in the diagnostic energy range with soft tissue. In fact, Compton scattering not only predominates in the diagnostic energy range above 26 kev in soft tissue, but continues to predominate well beyond diagnostic energies to approximately 30 Mev. This interaction is most likely to occur between photons and outer ("valence") shell electrons (Fig. 2.6). The electron is ejected from the atom, and the photon is scattered with some reduction in energy. As with all types of interactions, both energy and momentum must be conserved. Thus the energy of the incident photon (Eo) is equal to the sum of the energy of the scattered photon (Ese) and the kinetic energy of the ejected electron (Ee-), as shown in Equation.

$$E_{sc} = \frac{E_o}{1 + \frac{E_o}{511\ \text{keV}}(1 - \cos\theta)}$$

where E_{sc} = the energy of the scattered photon,
E_o = the incident photon energy, and
θ = the angle of the scattered photon.

The binding energy of the electron that was ejected is comparatively small and can be ignored (Bushberg et al.,2002).

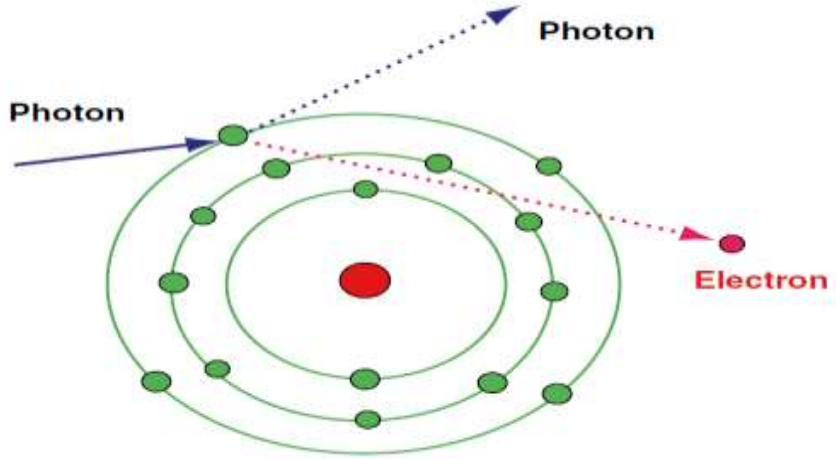

Figure (2-6) shows the Illustration of the Compton effect. (Murat, 2010).

Compton scattering results in the ionization of the atom and a division of the incident photon energy between the scattered photon and ejected electron. The ejected electron will lose its kinetic energy via excitation and ionization of atoms in the surrounding material. The Compton scattered photon may traverse the medium without interaction or may undergo subsequent interactions such as Compton scattering, photoelectric absorption (to be discussed shortly) (Bushberg et al.,2002).

The energy of the scattered photon can be calculated from the energy of the incident photon and the angle of the scattered photon (with respect to the incident trajectory):

2.2.5.1.2. Photoelectric effect:

In the photoelectric effect, all of the incident photon energy is transferred to an electron, which is ejected from the atom. The kinetic energy of the ejected

photo- electron (Ee) is equal to the incident photon energy (Eo) minus the binding energy of the orbital electron (Eb) .

$$E_e = E_o - E_b$$

In order for photoelectric absorption to occur, the incident photon energy must be greater than or equal to the binding energy of the electron that is ejected.

The ejected electron is most likely one whose binding energy is closest to, but less than, the incident photon energy. For example, for photons whose energies exceed the K-shell binding energy, photoelectric interactions with K-shell electrons are most probable. Following a photoelectric interaction, the atom is ionized, with an inner shell electron vacancy. This vacancy will be filled by an electron from a shell with a lower binding energy. This creates another vacancy, which, in turn, is filled by an electron from an even lower binding energy shell.Thus, an electron cascade from outer to inner shells occurs.

The difference in binding energy is released as either characteristic x-rays or auger electron. The probability of characteristic x-ray emission decreases as the atomic number of the absorber decreases and thus does not occur frequently for diagnostic energy photon interactions in soft tissue.

The probability of photoelectric absorption per unit mass is approximately proportional to Z3/E3, where Z is the atomic number and E is the energy of the incident photon. For example, the photoelectric interaction probability in

iodine (Z =53) is (53/20)3 or 18.6 times greater than in calcium (Z = 20) for photon of a particular energy.

The benefit of photoelectric absorption in x-ray transmission imaging is that there are no additional nonprimary photons to degrade the image. The fact that the probability of photoelectric interaction is proportional to 1/E3 explains, in part, why image contrast decreases when higher x-ray energies are used in the imaging process. If the photon energies are doubled, the probability of photoelectric interaction is decreased eightfold: ('/2)3 = 1/8.

Although the probability of the photoelectric effect decreases, in general, with increasing photon energy, there is an exception. For every element, a graph of the probability of the photoelectric effect, as a function of photon energy, exhibits sharp discontinuities called absorption edges.

The probability of interaction for photons of energy just above an absorption edge is much greater than that of photons of energy slightly below the edge. For example, a 33.2-keV x-ray photon is about six times as likely to have a photoelectric interaction with an iodine atom as a 33.1-keV photon **(Bushberg et al.,2002)**.

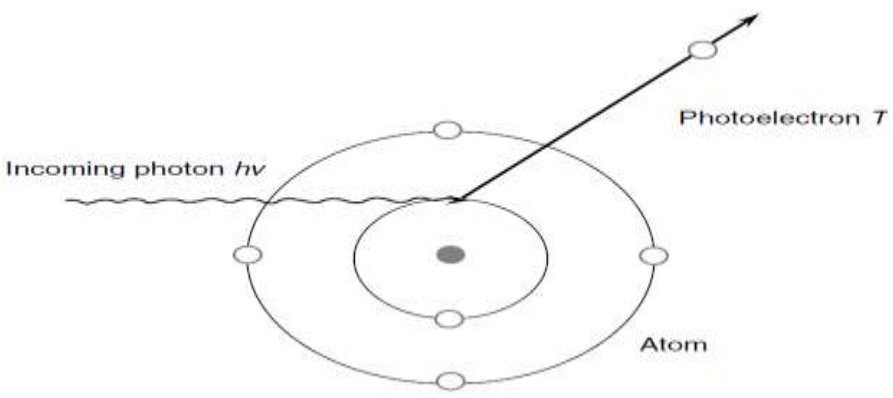

Figure (2-7) shows the Photoelectric absorption. An incoming photon with energy interacts with the atom and ejects a photoelectron with kinetic energy T. (P. MAYLES et al, 2007)

2.2.5.1.3. Pair production:

Pair production can only occur when the energies of x- and gamma rays exceed 1.02 MeV In pair production, an x-ray or gamma ray interacts with the electric field of the nucleus of an atom. The photon's energy is transformed into an electron-positron pair. The rest mass energy equivalent of each electron is 0.511 MeV and this is why the energy threshold for this reaction is 1.02 MeV. Photon energy in excess of this threshold is imparted to the electrons as kinetic energy. The electron and positron lose their kinetic energy via excitation and ionization. As discussed previously, when the positron comes to rest, it interacts with a negatively charged electron, resulting in the formation of two oppositely directed 0.511 MeV annihilation photons.

Pair production is of no consequence in diagnostic x-ray imaging because of the extremely high energies required for it to occur. In fact, pair production does not become significant unless the photon energies greatly exceed the 1.02 MeV energy threshold **(Bushberg et al.,2002)**

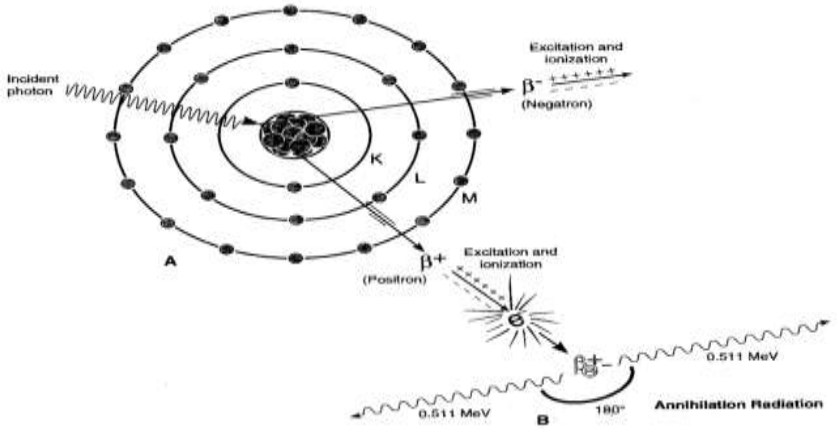

figure (2.8) show the Pair Production (Bushberg et al.,2002).

2.2.5.1.4. Coherent Effect (Rayleigh Scattering, Thomson Scattering):

Here, an electron is scattered when an electromagnetic wave or photon passes close to it. This type of scattering is explained by the waveform of the electromagnetic radiation. There are two types of coherent scattering: Thomson scattering and Rayleigh scattering (Fig. 2-9). The wave/photon only interacts with one electron in Thomson scattering, while it interacts with all of the electrons of the atom in Rayleigh scattering. (Murat, 2010).

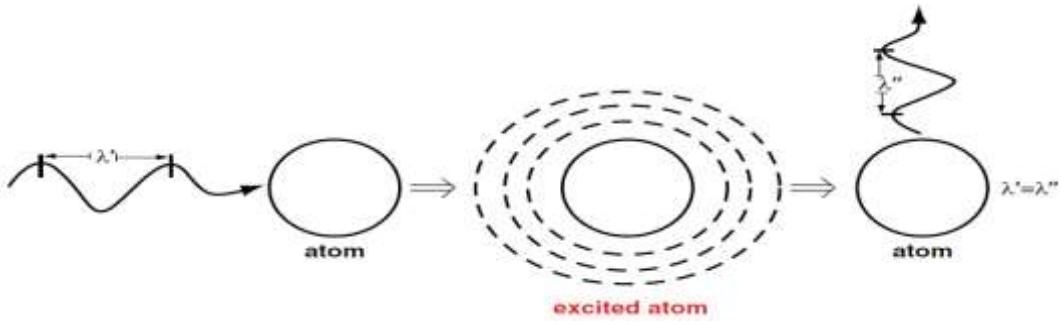

Figure (2-9) shows the Rayleigh scattering (Murat, 2010).

2.2.5.2. Interaction of Radiation with Polymeric Materials:

Polymeric substances respond to radiation in several ways, they can be gradually destroyed by UV radiation from sunshine when exposed for extended periods of time outdoors - more or less changing their properties. On the other hand, man-made UV radiation is actually used to produce polymers from monomers (low molecular weight building blocks for polymers) or from oligomers (essentially very low molecular weight polymers). Almost always in these reactions, a liquid is converted into a solid almost instantaneously. Ionizing radiation such as γ-rays and x-rays are even more versatile; it is capable of converting monomeric and oligomeric liquids into solids, but also

can produce major changes in properties of solid polymers. (Jiri George Drobny, 2003).

2.2.5.2.1. Cross-Linking and Chain Scission:

The most important reactions occurring during radiolysis of polymers are those that lead to permanent changes in their molecular weight. The reactions leading to either increases or decreases in molecular weight are referred to as cross-linking and chain scission, respectively. In general cross-linking and scission processes can occur simultaneously in any irradiated material; however, it is often observed that one tends to dominate over the other, and thus polymers can be broadly placed into the categories cross-linking or degrading. Some processes could be observed in irradiated polymer molecules, such as:

- **Evolution of gas**: When polymers are exposed to high energy radiation, the reactions induced will lead to the formation of low molecular weight gaseous molecules. For example, when polyethylene $-(-CH_2-)$ is irradiated, the scission of the C-H bond leads to the formation of thermally activated hydrogen atoms which are able to escape and form molecular hydrogen gas.

- **Formation of Unsaturated Groups**: When polymers are exposed to high energy radiation, chain scission leads to the formation of active atoms which lead to the evolution of gas and the formation of unsaturated groups. For example, the formation of main-chain unsaturation in irradiated polyethylene is proportional to the yield of hydrogen gas.

Color Centers: Most polymers change colors during irradiation. This change depends on the structure of the polymer, the irradiation temperature, the type of radiation and also varies for irradiations performed in vacuum and in air. The discoloration is attributed to the formation of conjugated double bonds in some polymers and also to trapped free radicals, electrons, and ion (DAVID J.T. HILL, et al., 2005).

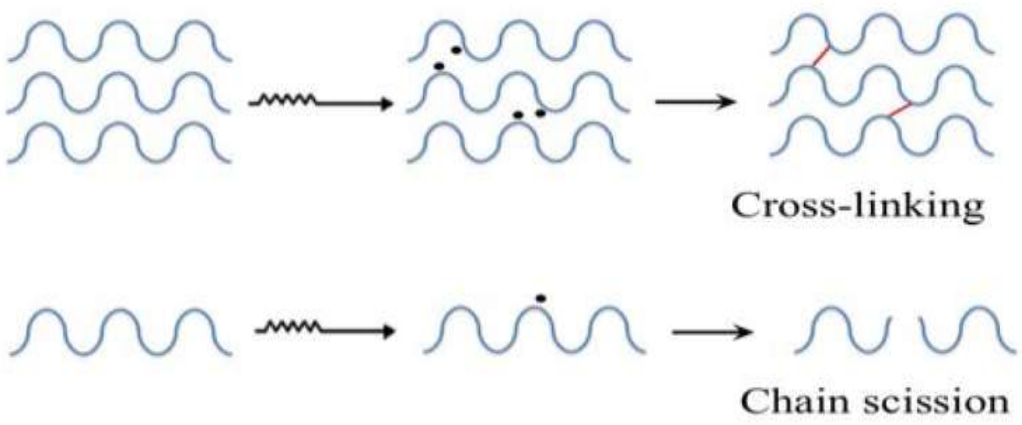

Figure (2-10) shows the Schematic representation of competing radiation induced polymer scission and cross-linking. **(Saphwan et al, 2016)**.

2.2.5.2.2. Radiation grafting:

Radiation grafting is a process in which active radical sites are formed on or near the surface of an exciting polymer, followed by polymerization of monomer on these sites. Grafting is accompanied by homo polymerization of the monomer; the material to which the monomer is grafted is described as the backbone, trunk or support. Radiation grafting is used to modify the polymers texture such as film, fibers, fabrics and molding powders.

The process of grafting can be expressed as follow; suppose the polymer A is

exposed to γ-rays, thus the active free radical sites A^* created randomly along the polymer backbone chain, this free radical initiate a free radical on the monomer B then undergoes grafting polymerization at that active sites. The extension of the attached monomer B upon the base polymer A is termed as the degree of grafting DOG which refers to the mass of the grafted polymer as a percentage of the mass of the original base polymer. Such process can be expressed in schematic Figure (2.11).

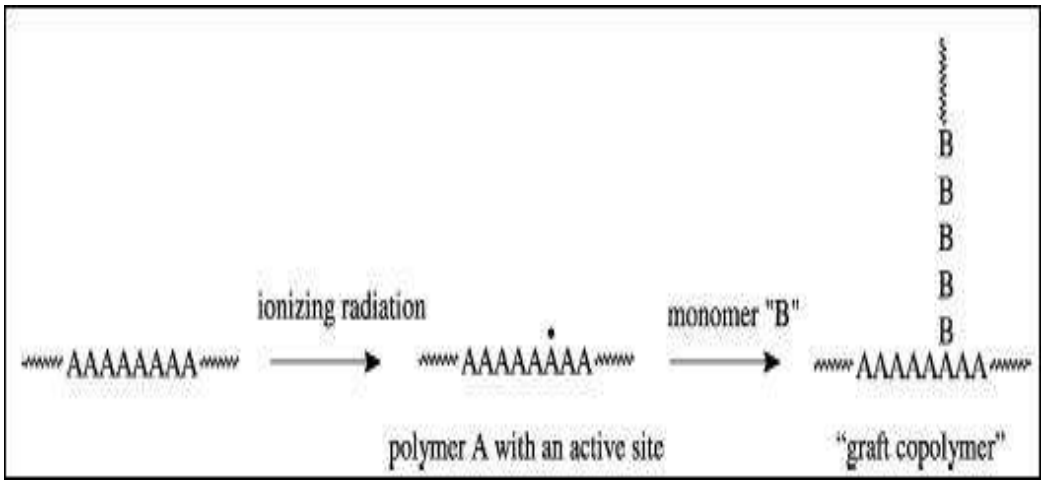

Figure (2-11) shows the schemes for grafting process for polymer A with monomer B using γ-radiation.

2.2.6. X-Ray Detectors:

The detection of x-ray is based on various methods. Before digital imaging was used the conventional film-screen system was the most commonly known method. Now a day this technique has been replaced by computed radiography (CR) and flat panel technology (HALL, E.J, 2002).

2.2.6.1. The modern film-screen detector:

System used for general radiography consists of cassette, one or two intensify screens, and a sheet of film. The film itself is a sheet of thin plastic with

photosensitive emulsion coated on to one or both sides. Film can be used to detect x-rays but it is relatively insensitive and therefore a lot of x-ray energy is required to produce a properly exposed x-ray film. To reduce the radiation dose to the patient, x-ray screens are used in all modern medical diagnostic radiography. Screens are made of a scintillation material, which is called a phosphor. When x-rays interact in phosphor, visible or ultraviolet (UV) light is emitted. This light given off by the screens that principally causes the film darkening; only about 5% of the darkening of the film is a result of direct x-ray interaction with the film emulsion. Therefore, film-screen detectors are considered an indirect detector. The emulsion of an exposed sheet of x-ray film is altered by the exposure to light and the latent image is recorded as altered chemical bonds in the emulsion, which are not visible. However, this latent image is visible during film processing (HALL, E.J, 2002).

2.2.6.2. Computed Radiography (CR):

is a term for photo stimulable phosphor detector (PSP) systems. Phosphors used in screen-film radiography, when x-ray are absorbed by photo stimulable phosphors, some light is emitted, but much of the absorbed x-ray energy is trapped in the PSP screen and can be read out later. For this reason, PSP screens are also called storage phosphors of imaging plates. CR was introduced in the 1970. After exposing the CR cassette is brought to CR reader. In the CR reader the imaging plate is scanned by laser beam. The laser light stimulates the emission of trapped energy in the imaging plate, and

visible light is released from the plate. To form the image, the light released from the plate is collected by photomultiplier tube (PMT) (HALL, E.J, 2002).

2.2.6.3. Flat panel detectors:

are newer detector technologies for computed radiography with fast-imaging capability. Two types of flat panel systems are used:

a- Indirect flat panel detectors are sensitive to visible light. An x-ray intensify screen is used to convert incident x-ray to light, which is then detected by photosensitive detector elements.

b- Direct flat panel detectors are made from a layer of photoconductor material. With direct detectors, the electrons released in the detector layer from x-ray interactions are used to form the image directly. Light photons from scintillation are not used (HALL, E.J, 2002).

2.2.7. Radiation dosimetry:

Radiation dosimetry is the calculation of the absorbed dose in matter and tissue resulting from the exposure to indirectly and directly ionizing radiation. It is a scientific subspecialty in the fields of health physics and medical physics that is focused on the calculation of internal and external doses from ionizing radiation.

2.2.7.1. Radiation quantities:

There are many different physical quantities that can be used to express the amount of radiation delivered to a human body. Generally, there are advantages and applications as well as disadvantages and limitations for each

of the quantities. There are two types of radiation quantities: those that express the concentration of radiation at some point, or to a specific tissue or organ, and there are also quantities that express the total radiation delivered to a body. We will be considering each of these quantities in much more detail (IAEA, 2005). The general relationship between the concentration and total radiation quantities are illustrated below.

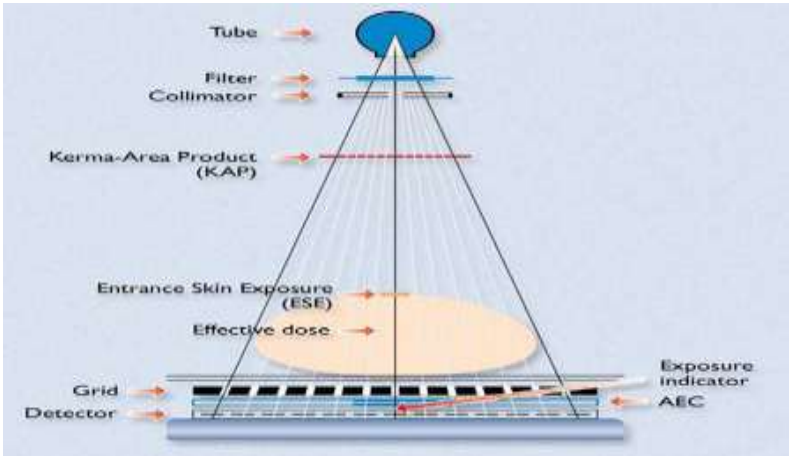

Figure (2.12) shows the typical examination beam geometry and related radiation dose quantities (IAEA, 2005)

2.2.7.1.1. Exposure:

Exposure is a radiation quantity that expresses the concentration of radiation delivered to a specific point, such as the surface of the human body. There are two units for expressing Exposure. The conventional unit is the roentgen (R) and the SI unit is the coulomb/kg of air (C/kg of air). The unit, the roentgen, is officially defined in terms of the amount of ionization produced in a specific quantity of air. The ionization process produces an electrical charge that is expressed in the unit of coulombs. So, by measuring the

amount of ionization (in coulombs) in a known quantity of air the exposure in roentgens can be determined (IAEA, 2005).

2.2.7.1.2. Air kerma:

Air kerma is a radiation quantity that is used to express the radiation concentration delivered to a point, such as the entrance surface of a patient's body. It is a quantity that fits into the SI scheme. The quantity, kerma, originated from the acronym, KERMA, for Kinetic Energy Released per unit Mass (of air). It is a measure of the amount of radiation energy, in the unit of joules (J), actually deposited in or absorbed in a unit mass (kg) of air. Therefore, the quantity, kerma, is expressed in the units of J/kg which is also the radiation unit, the gray (Gy) (IAEA, 2005).

2.2.7.1.3. Absorbed Dose:

Absorbed Dose is the radiation quantity used to express the concentration of radiation energy actually absorbed in a specific tissue. This is the quantity that is most directly related to biological effects. Dose values can be in the traditional unit of the rad or the SI unit of the gray (Gy). The rad is equivalent to 100 ergs of energy absorbed in a gram of tissue and the gray is one joule of energy absorbed per kilogram of tissue (IAEA, 2005).

2.2.7.1.4. Entrance Surface dose:

Entrance skin exposure is defined as the exposure in roentgens at the skin surface of the patient without the backscatter contribution from the patient. This measurement is popular because entrance skin exposure is easy to

measure, but unfortunately the entrance skin exposure is poorly suited for specifying the radiation received by patients undergoing radiographic examination. The entrance skin exposure does not take into account the radio sensitivity of individual organs or tissues, the area of an x-ray beam, or the beam's penetrating power, therefore, entrance skin exposure is poor indicator of the total energy imparted to the patient (NRPB, 2000).

2.2.7.1.5. Entrance surface air kerma (ESAK)

The entrance surface air kerma (ESAK) is defined as the kerma in air at the point where the central radiation beam axis enters the hypothetical object, i.e. patient or phantom, in the absence of the specified object (Zoetelief et al, 1996).

The entrance surface dose, or alternatively the entrance skin dose (ESD) is defined as the absorbed dose to air on the x-ray beam axis at the point where x-ray beam enters the patient or a phantom, including the contribution of the backscatter (NRPB, 1992). The ESD is to be expressed in mGy. Some confusion exists in the literature with regard to the definition of the ESD. That is, whether the definition should refer to the absorbed dose to the air as defined above or absorbed dose to tissue (NRPB, 2000).

2.2.7.1.6. Equivalent dose H_T:

Accounts for biological effect per unit dose

$$HT = WRxD$$

2.2.7.1.7. Effective dose E:

Risk related parameter, taking relative *radio sensitivity* of each organ and tissue into a count:

$$E(Sv)= \Sigma_T W_T \times H_T$$

W_T: tissue weighting factor for organ T

H_T: equivalent dose received by organ or tissue T

2.2.7.2. Radiation Units:

2.2.7.2.1. Roentgen:

The roentgen is a unit used to measure a quantity called exposure. This can only be used to describe an amount of gamma and X-rays, and only in air. One roentgen is equal to depositing in dry air enough energy to cause 2.58 x 10-4 coulombs per kg. It is a measure of the ionizations of the molecules in a mass of air. The main advantage of this unit is that it is easy to measure directly, but it is limited because it is only for deposition in air, and only for gamma and x-rays (Avenue, 2002).

2.2.7.2.2. Radiation absorbed dose (Rad):

The rad is a unit used to measure a quantity called absorbed dose. This relates to the amount of energy actually absorbed in some material, and is used for any type of radiation and any material. One rad is defined as the absorption of 100 ergs per gram of material. The unit rad can be used for any type of

radiation, but it does not describe the biological effects of the different radiations (Avenue, 2002).

2.2.7.2.3. Rem (roentgen equivalent man):

The rem is a unit used to derive a quantity called equivalent dose. This relates the absorbed dose in human tissue to the effective biological damage of the radiation. Not all radiation has the same biological effect, even for the same amount of absorbed dose. Equivalent dose is often expressed in terms of thousandths of a rem, or m rem. To determine equivalent dose (rem), you multiply absorbed dose (rad) by a quality factor (Q) that is unique to the type of incident radiation.

2.2.7.2.4. Gray (Gy):

The gray is a unit used to measure a quantity called absorbed dose. This relates to the amount of energy actually absorbed in some material, and is used for any type of radiation and any material. One gray is equal to one joule of energy deposited in one kg of a material. The unit gray can be used for any type of radiation, but it does not describe the biological effects of the different radiations. Absorbed dose is often expressed in terms of hundredths of a gray, or centi-grays. One gray is equivalent to 100 rads.

2.2.7.2.5. Sievert (Sv):

The sievert is a unit used to derive a quantity called equivalent dose. This relates the absorbed dose in human tissue to the effective biological damage

of the radiation. Not all radiation has the same biological effect, even for the same amount of absorbed dose. Equivalent dose is often expressed in terms of millionths of a sievert, or micro-sievert. To determine equivalent dose (Sv), you multiply absorbed dose (Gy) by a quality factor (Q) that is unique to the type of incident radiation. One sievert is equivalent to 100 rem (Thayalan,2001).

2.2.8. Radiation measurements:

X-ray detectors convert the transmitted X-rays into useful, measurable signals. Solid state detectors contain crystals whose atoms are arranged in a regular three dimensional structure. When X-rays interact with atoms in the detector, energy is transferred to the electrons and is handled according to the type of detector. In a screen-film detector, the deposited energy is converted into multiple visible light photons that travel through the screen, depositing energy in the film grains found in the emulsion layers of the film. The image is stored in the film emulsion. Screen-film images can be converted into a digital format using a film digitizer (Williams et al., 2007). In the photo stimulable phosphors used in computed radiography (CR), the energy is stored and can be read out by light stimulation. The CR plates are read out pixel-by-pixel using a laser and the image can be stored on a computer, printed on film or viewed on a monitor. Digital flat panel detectors can be classified into direct and indirect systems (Boone, 2000; Huda, 2010; Williams et al., 2007). Direct systems such as photoconductors produce an

electronic signal that is proportional to the deposited energy and can be directly measured (Huda, 2010). Indirect detectors make use of scintillators that convert the deposited energy into light which is subsequently propagated to a photodetector through optic diffusion. The photo detector records the pattern of visible light emitted by the scintillator as an image (Boone, 2000).

With respect to measurement, three separate features of an X-ray beam must be identified. The first consideration is the flux of photons travelling through air from the anode towards the patient. The ionization produced by this flux is a measure of the Radiation exposure. If expressed per unit area per second it is the intensity of more fundamental importance as far as the biological risk is concerned is the absorbed dose of radiation. This is a measure of the amount of energy deposited as a result of ionization processes.

2.2.8.1 Dose measurement:

There are several ways of measuring doses from ionizing radiation. Workers who come in contact with radioactive substances or may be exposed to radiation routinely carry personal dosimeters. In the United States, these dosimeters usually contain materials that can be used in thermoluminescent dosimeter (TLD) or optically stimulated luminescence (OSL). Outside the United States, the most widely used type of personal dosimeter is the film badge dosimeter, which uses photographic emulsions that are sensitive to ionizing radiation. The equipment used in radiotherapy (linear particle

accelerator in external beam therapy) is routinely calibrated using ionization chambers or the new and more accurate diode technology (EPA, 2006).

2.2.8.1.1. Ionization chamber:

In medical x-ray imaging the Free-in-air air kerma measurements are best made with suitably designed ionization chambers of typically between 0.6 and 180 cm3 volume. The chambers should have 'air equivalent' walls so that their energy response in terms of air kerma is substantially uniform for all relevant x-ray spectra. The leakage current should be very small compared with the ionization current produced by the minimum dose rate to be measured and the response should not be affected appreciably by ion recombination at high dose rates. Dosimeters should be calibrated in a manner traceable to a national primary standard of air kerma as described; there are special requirements for ionization chambers used for air-kerma measurements in mammography: these are a thin entrance wall to reduce attenuation at low photon energies, and ideally a structure that does not appreciably disturb the primary radiation field. Thin entrance window chambers with small volumes generally have a rather massive construction on the exit side, which implies that the charge produced in the cavity contains a significant contribution from scattered radiation (HALL, 2002).

2.2.8.1.2. Dose -area product meters:

Dose area product is defined as the absorbed dose to air averaged over the area of the X-ray beam in a plane perpendicular to the beam axis multiplied by the area of the beam in the same plane. It is usually measured on Gy cm2 and radiation backscattered from the patient is excluded Provided that the cross sectional area of the beam lies completely within the detector, it may be shown by simple application of the inverse square law that the reading will not vary with the distance from the tube focus.

Thus the dose area product can be measured at any point between the diaphragm housing on the X-ray tube and the patient, but not so close to the patient that there is significant backscattered radiation. Dose area product meters consist of flat, large area parallel plate ionization chambers connected to suitable electrometers which respond to total charge collected over the whole area of the chamber. The meter is mounted close to the tube focus where the area of the X-ray beam is relatively small and dose rates are high. It is normally mounted on the diaphragm housing where it does not interfere with the examination and is usually transparent so that when fitted to an over –couch X-ray tube the light beam diaphragm device can still be used (Avenue, 2002).

2.2.8.1.3. Thermo Luminescent Dosimetry:

Many crystalline materials exhibit phenomena of thermo luminescence. When such a crystal is irradiated, a very minute fraction of the absorbed energy is stored in crystal lattice. Some of this energy can be recovered latter as visible

light if the material is heated. This phenomena of release of visible photon by thermal means is known as thermos luminescence. (Thayland, 2001).

2.2.8.1.4. Radiochromic Dosimetry:

Radiochromic film is a new type of film in radiotherapy dosimetry. The most commonly used is a GafChromic film. It is a colorless film with a nearly tissue equivalent composition (9.0% hydrogen, 60.6% carbon, 11.2% nitrogen and 19.2% oxygen) that develops a blue color upon radiation exposure. Radiochromic film contains a special dye that is polymerized upon exposure to radiation. The polymer absorbs light, and the transmission of light through the film can be measured with a suitable densitometer. Radiochromic film is self-developing, requiring neither developer nor fixer. Since radiochromic film is grainless, it has a very high resolution and can be used in high dose gradient regions for dosimetry (e.g. measurements of dose distributions in stereotactic fields and in the vicinity of brachytherapy sources).

Dosimetry with radiochromic films has a few advantages over radiographic films, such as ease of use; elimination of the need for darkroom facilities, film cassettes or film processing; dose rate independence; better energy characteristics (except for low energy X rays of 25 kV or less); and insensitivity to ambient conditions (although excessive humidity should be avoided). Radiochromic films are generally less sensitive than radiographic films and are useful at higher doses, although the dose response non-linearity should be corrected for in the upper dose region.

● Radiochromic film is a relative dosimeter. If proper care is taken with calibration and the environmental conditions, a precision better than 3% is achievable.

● Data on the various characteristics of radiochromic films (e.g. sensitivity, linearity, uniformity, reproducibility and post-irradiation stability) are available in the literature (E.B. Podgorsak, 2005).

2.3. Polymers:

Polymers are organic compounds of high molecular weight formed by small molecules, monomers, linked together. one of the characteristics of a good 3D dosimeter is being solid. The hardening of a polymer is called curing. This term includes polymerization (link of monomers) and cross-linking (link of polymer chains) *(Drobny, 2010).*

One of the indicators of the progress of human civilization is the type of materials that are accessible to society. Just as the Metal (Bronze and Iron) Age marked the beginning of a new chapter of human civilization at the end of the Stone Age, the advent of polymers in the last century has heralded a new era. Conventional materials such as iron, steel, wood, glass or ceramics are today being either supplemented or replaced by polymeric materials *(Vadapalli Chandrasekhar, 2005)*

2.3.1. Polymer properties:

Polymer properties are broadly divided into several classes based on the scale at which the property is defined as well as upon its physical basis. (S.A.

Baeurle, 2009). The most basic property of a polymer is the identity of its constituent monomers. A second set of properties, known as microstructure, essentially describe the arrangement of these monomers within the polymer at the scale of a single chain. These basic structural properties play a major role in determining bulk physical properties of the polymer, which describe how the polymer behaves as a continuous macroscopic material. Chemical properties, at the nano-scale, describe how the chains interact through various physical forces. At the macro-scale, they describe how the bulk polymer interacts with other chemicals and solvents.

2.3.2. Polymerization:

Radiation polymerization is a process in which the free radicals interact with the unsaturated molecules of a low molecular unit known as monomer to form high molecular mass polymer or even with different monomers to produce crosslink polymer. The formed polymer can be in different forms called homo polymer and copolymer depending on the monomer compositions link together.

Radiation-induced polymerization process can be achieved in different media whether it is liquid or solid unlike the chemical polymerization which can only accomplished in aqueous media. It is also temperature independent. Radiation polymerization often continues even after removing away from the radiation source. Such condition is known as post-polymerization (Lokhovitsky and Polikarpov, 1980). Since radiation initiation is temperature independent, polymer can be polymerized in the frozen state around aqueous

crystals. The mechanism of the radiation induced polymerization is concerning the kinetics of diffusion-controlled reactions and consists of several stages: addition of hydroxyl radicals and hydrogen atoms to carbon-carbon double bond of monomer with subsequent formation of monomer radicals; addition of hydrated electrons to carbonyl groups and formation of radical anion of a very high rate constant and the decay of radicals with parallel addition of monomer to the growing chain.

2.3.3. Polyvinyl alcohol (PVA)

PVA is one of the important polymer binder and available in the form of powders, fibers and films. It can be obtained from poly (vinyl acetate) (PVAc) by esterification and has distinct crystallinity. The polymer has intermolecular chin of 2.5 Å and consists of 1,3 glycol linkages, in which all hydroxyl groups are arranged along the same side of the chain. These in turn account for the mechanical strength and strong interactions between different chains. The unit cell of PVA consists of two monomer units of vinyl alcohol (CH_2CHOH) (Bunn, 1948) as in Fig. (2-13).

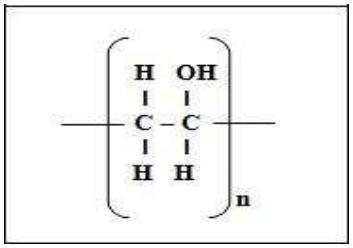

Figure (2-13) shows the Chemical structure of poly (vinyl alcohol) (PVA) monomer.

It is non-ionic vinyl polymer, tough with film forming capacity due to hydrogen bonding (Ravve, 2000), fibres and tubes forming capability and highly resistant to hydrocarbon solvents (Molyneux, 1983). It is highly resistive to electrical conductivity with low dielectric loss. Its electrical

conductivity and charge storage capability can be significantly influence by doping with suitable impurities (Nagaraja, *et al*., 2002). Due to biocompatibility, PVA has been used in medical devises, materials for drug delivery system, carrier for cell signaling, sizing, adhesives, emulsification and bio-separation membranes (Yano, *et al.*, 2003).

2.4. Silver Nitrate ($AgNO_3$):

Silver nitrate is a chemical compound with a chemical formula $AgNO_3$ shown in Figure 3.2. This nitrate of silver is the light sensitive ingredient in photographic film and is a corrosive compound. Soluble silver salts tend to be very toxic to bacteria and other lower life species. The compound notably stains the skin giving a blackening color which is made visible after exposure to sunlight. Silver nitrate is one of the significant compounds in the field of industries due to its potential characteristics such as wider response to electromagnetic radiations i.e. optical properties in addition to electronic, magnetic and catalysis (Wang and Toshima, 1997). It has been used in wider applications as conductive ink, thick film pastes, adhesive for electronic compounds (Lin and Wang, 1996) and photonic and photographic applications (Jin et al., 2001). The characteristics of silver nitrate are has a molecular weight of 169.87, boiling point 444 ^oC, melting point 212 ^oC as crystal structure rhombic, decomposed by heat to give Ag, NO_2 and O_2.

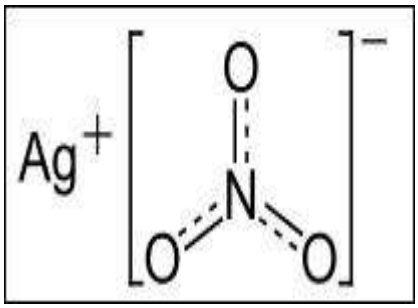

Figure (2.14) shows The chemical structure of the silver nitrate compound.

2.5. Absorption of light and UV-Visible spectrophotometry:

2.5.1. Wavelength and frequency:

Electromagnetic radiation can be considered a combination of alternating electric and magnetic fields that travel through space with a wave motion. Because radiation acts as a wave, it can be classified in terms of either wavelength or frequency, which are related by the following equation:

$$\nu = c / \lambda$$

where n is frequency (in seconds), c is the speed of light (3 × 108 ms-1), and l is wavelength (in meters). In UV-visible spectroscopy, wavelength usually is expressed in nanometers (1 nm = 10-9 m).

It follows from the above equations that radiation with shorter wavelength has higher energy. In UV-visible spectroscopy, the low-wavelength UV light has the highest energy. In some cases, this energy is sufficient to cause unwanted photochemical reactions when measuring sample spectra (remember, it is the UV component of light that causes sunburn). (A Primer, 1996).

2.5.2. Origin of UV-visible spectra:

When radiation interacts with matter, a number of processes can occur, including reflection, scattering, absorbance, fluorescence/phosphorescence (absorption and reemission), and photochemical reaction (absorbance and bond breaking). In general, when measuring UV-visible spectra, we want only absorbance to occur. Because light is a form of energy, absorption of light by matter causes the energy content of the molecules (or atoms) to increase.

The total potential energy of a molecule generally is represented as the sum of its electronic, vibrational, and rotational energies:

$$E_{\text{total}} = E_{\text{electronic}} + E_{\text{vibrational}} + E_{\text{rotational}}$$

The amount of energy a molecule possesses in each form is not a continuum but a series of discrete levels or states. The differences in energy among the different states are in the order:

$$E_{\text{electronic}} > E_{\text{vibrational}} > E_{\text{rotational}}$$

In some molecules and atoms, photons of UV and visible light have enough energy to cause transitions between the different electronic energy levels. The wavelength of light absorbed is that having the energy required to move an electron from a lower energy level to a higher energy level. (A Primer, 1996).

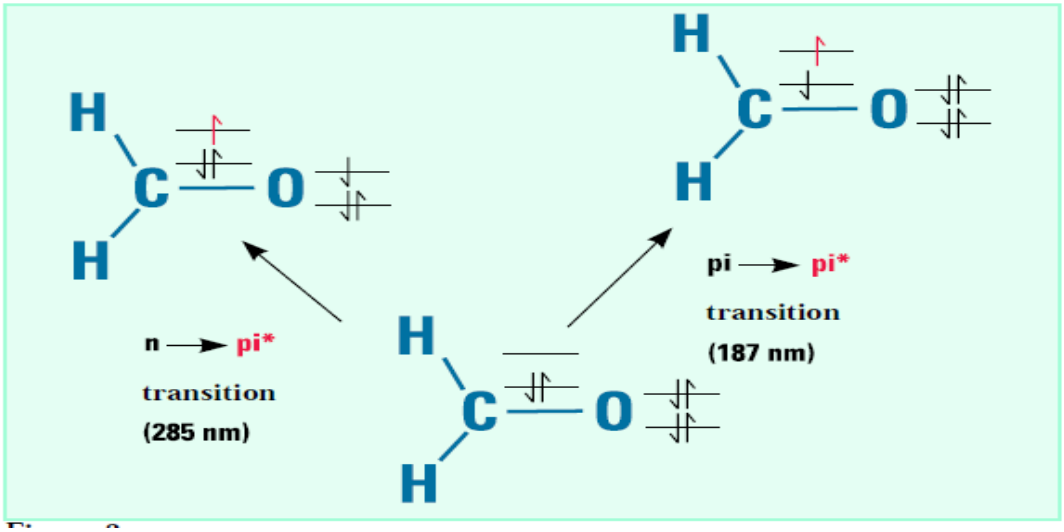

Figure (2-15) shows an example of electronic transitions in formaldehyde and the wavelengths of light that cause them. (A Primer, 1996).

These transitions should result in very narrow absorbance bands at wavelengths highly characteristic of the difference in energy levels of the absorbing species. This is true for atoms, as depicted in Figure (2-16).

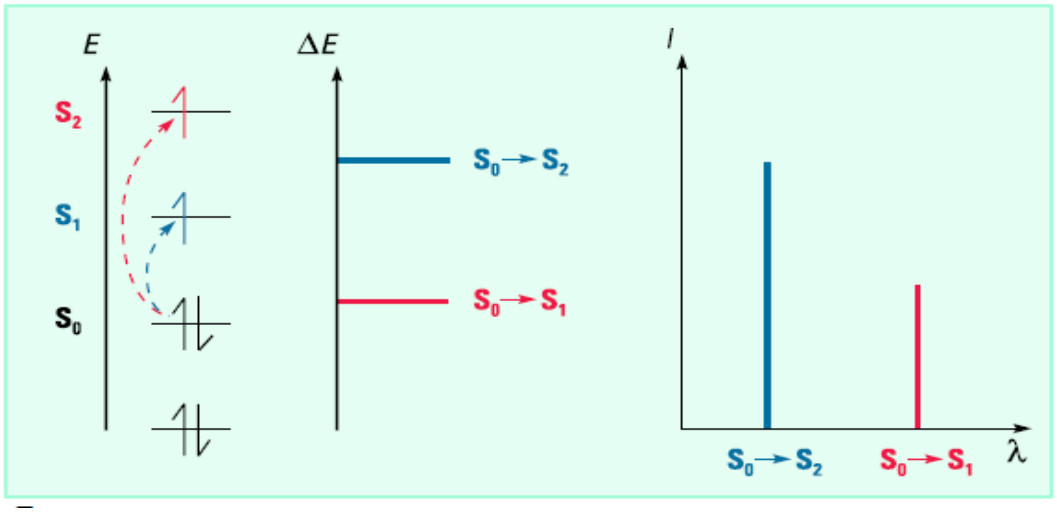

Figure (2-16) shows the Electronic transitions and spectra of atoms. (A Primer, 1996).

However, for molecules, vibrational and rotational energy levels are superimposed on the electronic energy levels. Because many transitions with

different energies can occur, the bands are broadened. The broadening is even greater in solutions owing to solvent-solute interactions. (A Primer, 1996).

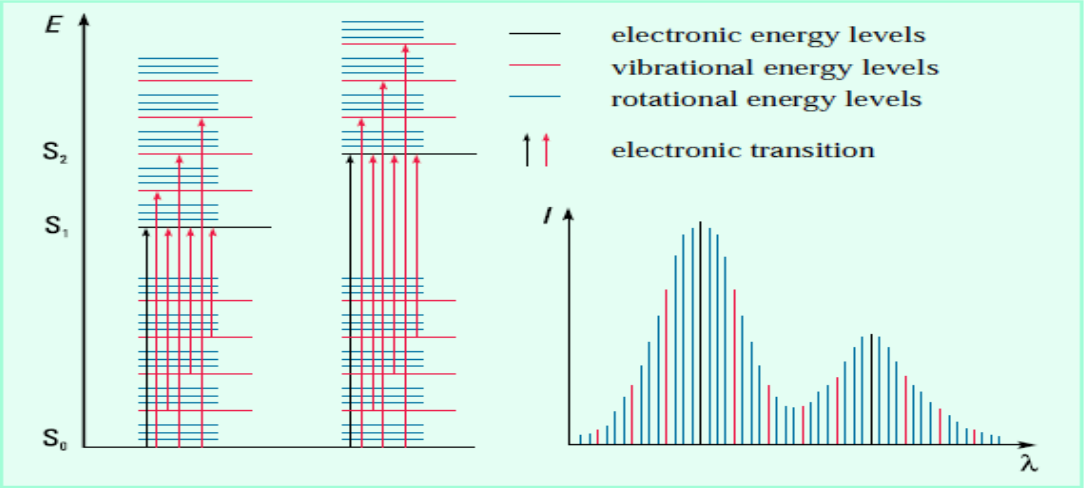

Figure (2-17) shows the Electronic transitions and UV-visible spectra in molecules. (A Primer, 1996).

2.5.3. Optics of spectrophotometer:

Either lenses or concave mirrors are used to relay and focus light through the instrument. Simple lenses are inexpensive but suffer from chromatic aberration, that is, light of different wavelengths is not focused at exactly the same point in space. However, with careful design, the chromatic aberrations of individual lenses in an optical system can be used to cancel each other out, and an effective optical system can be constructed with these simple and inexpensive components. Achromatic lenses combine multiple lenses of different glass with different refractive indices in a compound lens that is largely free of chromatic aberration. Such lenses are used in cameras. They offer good performance but at relatively high cost. Concave mirrors are less expensive to manufacture than achromatic lenses and are completely free of

chromatic aberration. However, the aluminum surface is easily corroded, resulting in a loss of efficiency. At each optical surface, including the interfaces between components in an achromatic lens, 5–10 % of the light is lost through absorbance or reflection. Thus spectrophotometers ideally should be designed with a minimum number of optical surfaces. (A Primer, 1996).

2.5.4. conventional spectrophotometer:

Figure (2-18) shows a schematic of a conventional single-beam spectrophotometer. Polychromatic light from the source is focused on the entrance slit of a mono chromator, which selectively transmits a narrow band of light. This light then passes through the sample area to the detector. The absorbance of a sample is determined by measuring the intensity of light reaching the detector without the sample (the blank) and comparing it with the intensity of light reaching the detector after passing through the sample. As discussed above, most spectrophotometers contain two source lamps, a deuterium lamp and a tungsten lamp, and use either photomultiplier tubes or, more recently, photodiodes as detectors. (A Primer, 1996).

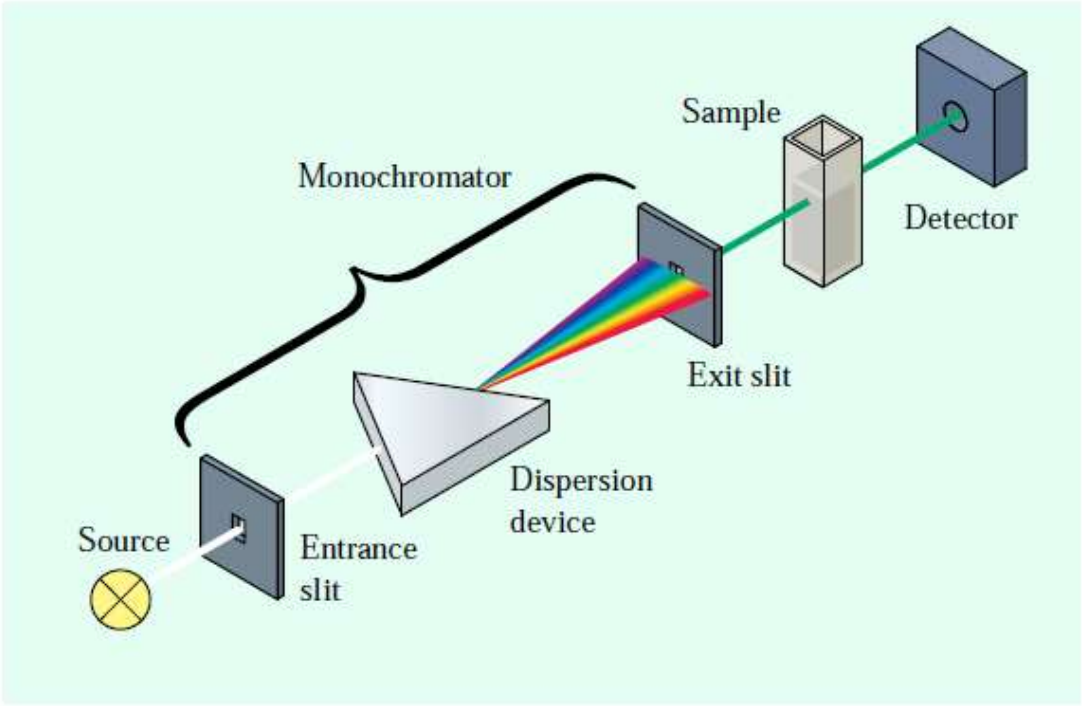

Figure (2-18) shows the Schematic of a conventional spectrophotometer (A Primer, 1996). This design is well-suited for measuring absorbance at a single point in the spectrum. It is less appropriate, however, for measuring different compounds at different wavelengths or for obtaining spectra of samples. To perform such tasks with a conventional spectrophotometer, parts of the mono chromator must be rotated, which introduces the problem of mechanical irreproducibility into the measurements. Moreover, serial data acquisition is an inherently slow process. (A Primer, 1996).

2.5.5. The diode array spectrophotometer:

Figure (2-19) shows a schematic diagram of a diode array spectrophotometer. Polychromatic light from a source is passed through the sample area and focused on the entrance slit of the poly chromator. The poly chromator disperses the light onto a diode array, on which each diode measures a narrow

band of the spectrum. The bandwidth of light detected by a diode is related to the size of the poly chromator entrance slit and to the size of the diode. Each diode in effect performs the same function as the exit slit of a mono chromator (A Primer, 1996).

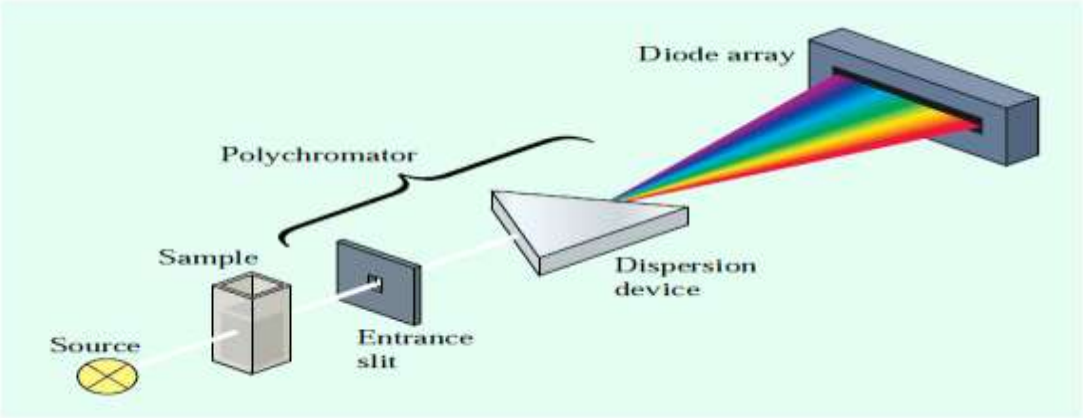

Figure (2-19) shows the **Schematic of a diode array spectrophotometer** **(A Primer, 1996).**

2.6. Previous studies:

For the wider interested applications of polymer hybridized metal nanoparticles composites, poly vinyl-alcohol/silver nanoparticles composites in a form of a film was prepared by in situ irradiation doping technique up to 50 kGy. The effect of radiation upon the composites resulted in reducing the silver ions into black metallic silver, so the general film color changed from white to golden-yellow then black color at 50 kGy. The UV-Vis spectroscopy revealed an absorbance band peaking at 425 nm which was increased exponentially with dose increment. The study of UV-spectrogram revealed that the maximum absorbance Amax increased following the particles radius. Scanning electron Microscopy (SEM) revealed shiny nanoparticles of silver

cored in Polyvinyl-alcohol PVA with homogeneous distribution and having an average size of 30 nm as well as the XRD spectrum that shows cubic center face of silver nanoparticles in the film and a crystalline peak for PVA reduced by radiation to amorphous phase **(Omer M., et al., 2011).**

the Dosimetric characterization and spectroscopic study of radiochromic films as natural dye dosimeters, Radiochromic films were prepared with PVA gel matrix and natural dyes (Turmeric, Walnut and Henna) with three concentrations, that is, C1=0.5 g/L, C2=0.25 g/L and C3=0.13 g/L having pH value 4 for acidic samples and 10 for alkaline samples. The thickness of the film was fixed to be 0.05 mm. The behavior of the dyes was studied on the basis of change in specific absorbance with concentration, change in specific absorbance with absorbed dose; effect of pH on specific absorbance, electrical conductivity, molar extinction coefficients, and percentage decoloration. Absorption spectra for un-irradiated and Gamma irradiated films were studied. ʎmax for T= 451 nm, for W=340 nm and for H=320 nm was recorded. Absorbance at each ʎmax was found by using spectrophotometer and specific absorbance was calculated. Response curve for specific absorbance versus concentration showed linear behavior for each dye. Plot of specific absorbance versus dose made the behavior of the dye clear and it was noticed that acidic samples of all the dye samples worked best. Maximum degree of decoloration in the Turmeric, Walnut and Henna dye films was observed to be 94%, 51.5% and 93.7% respectively. XRD analysis was

performed and it was found that for Turmeric, %age crystallanity as well as C.I decreased while for Walnut and Henna both factors increased. Moreover, mechanical properties of dye films were studied which showed that due to irradiation some changes had occurred in the crystal structure which is the major reason of decoloration of the dye films. (**Muhammad Attique et al, 2014).**

The effects of gamma irradiation on optical properties of cresol-red dyed Poly Vinyl Alcohol (PVA) blended with Trichloroacetic Acid (TCA) for possible use in dosimetry and measurement of radiation dose in gamma rays have been studied using both Raman spectroscopy and UV-Visible spectrophotometer method, the dosimeters are composed of Poly Vinyl Alcohol (PVA), Trichloroacetic Acid (TCA) at various concentrations are 20, 25, 30 and 35%, and acid-base indicator cresol-red dyed. The dosimeters were irradiated to doses up 12 kGy using 60Co gamma ray source at a constant dose rate. The polymeric films undergo color change from purple to yellow due to radiation-induced acid formation. The molecular vibrational spectra were measured using Raman spectroscopy, resulting in a decrease of the Raman intensity inelastic scattering of C-Cl molecular stretching from TCA with increasing dose. The absorption spectra were measured using UV-visible spectrophotometer in the wavelength range 350-700 nm, resulting in a decrease of the absorbance at 575 nm band peak with increasing dose. The dose sensitivity D0 increases with increasing TCA concentration for both

scattering and absorption methods. The optical absorption studies show that the direct and indirect optical energy band gaps and optical activation energies are dependent on dose and TCA concentration. The shift in the optical band gap Eg values towards lower energy with radiation dose leads to a shift of the optical activation energy Delta E value towards the lower energy region with increasing dose. The optical band gap (Eg) and the absorption edge decrease with increasing dose attributed to the structural disorder of polymer blends due to dehydrochlorination of trichloroacetic acid with increasing dose. The energy width of the tail of localized state in the forbidden band gap was evaluated using the Urbach-edges method. It was found that the activation energy (Delta E) is less dependent of radiation dose but strongly dependent on concentration of blends. **(Susilawati et al, 2009).**

The investigation of film dosimeters made from polyvinyl alcohol (PVA) films dyed with methyl orange (MO) to enable their use in high dose radiation processing applications was studied. The dosimetric change in these films at pre and post irradiation was studied spectrophotometrically. Radiolytic bleaching was observed in PVA aided films exposed with Cs137 ɤ-source in dose range of 100-200kGy. The effects of pH, dye concentration and film thickness on the radiation response of the film dosimeters were discussed. The stability of MO-PVA films before and after exposure of radiation was also examined at ambient temperature and was found to be higher for long times at pre and post irradiation stages. The preliminary study on the PVA based films

containing methyl orange dye indicates that radiation induced decoloration of these films can be used for dosimetry. The results indicate that the response of these films depends on the absorbed dose, dye concentration, pH and film thickness. The MO-PVA film is highly stable for long times before and after irradiation. PVA based films are easy to make and do not require toxic solvents in the preparation therefore, these are amenable for large-scale production and application for routine irradiation processes of medical equipment. **(Shaheen Akhtar et al, 2013).**

polyaniline (PANI) and nickel (Ni) nanoparticles embedded in polyvinyl alcohol (PVA) film matrix was made by gamma radiolytic method. The mechanism of formation of PANI and Ni nanoparticles were proposed via oxidation of aniline and reduction of Ni ions, respectively. The effects of dose and Ni ions concentration on structural, optical, and electrical properties of the final PVA/PANI/Ni nanocomposites film were carefully examined. The structural and morphological studies show the presence of PANI with irregular granular microstructure and Ni nanoparticles with spherical shape and diameter less than 60 nm. The average particle size of Ni nanoparticles decreased with increasing dose and decreasing of precursor concentration due to increase of nucleation process over aggregation process during gamma irradiation. The optical absorption spectra showed that the absorption peak of Ni nanoparticles at about 390 nm shifted to lower wavelength and the absorbance increased with increasing dose. The formation of PANI was also

revealed at 730 nm absorption peak with the absorbance increasing by the increase of dose. The electrical conductivity increased with increasing of dose and chlorine concentration due to number of polarons formation increases in the PVA/PANI/Ni nanocomposites. Optical absorption spectra show a blue shift of the absorption peak of Ni nanoparticles due to decreasing particle size with increasing of dose. The optical band gap of PANI decreased with increasing of dose and chlorine concentration. Moreover, the absorbance of both PANI and Ni nanoparticles increased with dose due to increase of polarons and Ni nanoparticles formation. Finally, the electrical conductivity of the nanocomposites increased with the increase of dose and chlorine concentration corresponds to the increased amount of polarons. **(Abdo Mohd et al, 2014)**.

study was done to evaluate the effect of photon on the optical properties of dyed polyvinyl alcohol-trichloroacetic acid (PVA-TCA) blends prepared through solvent casting technique at radiotherapy dose. The films were cut into 2 × 2 cm2 and kept away from direct sunlight at room temperature until irradiation process. The films were simultaneously irradiated with a 6 MV photon beam produced by linear accelerator Siemens MXE-2. The dose exposure given was set from 50 to 400 cGy. The optical properties were measured using the UV-visible spectrophotometer Shimadzu-1800, set at a wavelength range between 200 nm and 800 nm. The absorbance spectra were obtained with the existence of three absorbance band peaks at 273 nm, 444

nm and 582 nm. Initially, all absorbance increased with increasing dose applied. The results gained indicate that the optical energy band gap, Eg is equivalent to 5.20 eV while the absorption edge is 4.96 eV. These two parameters decreased with increasing dose. It is due to the increase of structural order between the conduction band and the valence band getting narrower. This also indicates that the film is undergoing a red shift. Hence, the value of Urbach energy, ΔE obtained is 0.089 eV, which increased with increasing dose since the lattice vibration depended on the applied dose. In conclusion, the PVA/TCA blends have a good optical characteristic in terms of dose response and optical transition. **(Iskandar, et al, 2013)**

Silver-doped PVA films were prepared by casting method in order to study the effect of silver on the optical properties of poly (vinyl alcohol) using UV/VIS spectroscopy. PVA with molecular weight of 10000 g/mol (BDH chemicals England) was used as the basic polymeric materials in this work. The PVA solution films with different amounts of AgNO3 dopant were prepared by solution casting method. 1 g of PVA powder was added to doubly distilled water and allowed to swell for 24 h at room temperature. Silver nitrate was dissolved in redistilled water and added to the polymeric solution with continuous stirring. Then the solution was poured into flat glass plate dishes. Homogenous films were obtained after drying in an air oven for 24 h at 40 C. The thickness of the films were in the range of 20 ± 0.05 μm. The optical studies were carried out using double bean spectrometer (Shimadzu

UV probe Japan) in the wavelength range (300-900) nm and infrared spectra were recorded using Shimadzu FTIR-8700 spectrometer in the wavelength range (400-4000) cm-1 with a resolution of 4 cm-1. It was found that these thin films have an indirect optical band gap (2.4-1.3) eV as the doping percentage increase. Extinction coefficient and refractive index increase as the doping percentage increase, while in general the optical dispersion parameters show an opposite behavior with doping. **(W.A. Jabbar, et al, 2010).**

study was by **Mohammed A. Ali Omer,** to synthesize PVA\AgNO3 polymer films and to optimize it is radiation measurement based on entrance and exit dose measurement relative to thermoluminiscence detector (TLD) method. The polymer films have been synthesized by casting technique after dissolving of polyvinyl alcohol (PVA) under controlled temperature (80 ^{o}C) and stirring and hybridization with silver nitrate (AgNO3). The polymer films have been characterized after irradiation at the entrance and exit sites of Perspex by UV-visible spectroscopy and an optical densitometer (OD). The study revealed that there were absorption peaks at wavelength 190 and 425 nm related to pure PVA and silver out of UV-visible spectroscope, and the average entrance and exit doses read by TLD was 7.06±4.7 and 3.98±2.8 Gy and they are usually less than the applied dose by an average factor of 0.22 and 3.3 Gy respectively, also there is a linear proportional and significant (R2 = 0.9) relationship between the applied dose and the measured OD at entrance and exit side of the phantom that could be fitted in the following equation: y =

0.040x + 0.117 and y = 0.031x + 0.099 respectively, where x refers to the applied dose and y refers to the OD at the entrance and exit sides of the phantom. Also there is a linear proportional and significant (R2 = 0.9) relationship between the entrance\exit doses measured by TLD and the relative OD at both sides of the phantom which could be fitted in the following equation: y = 0.035x + 0.159 and y = 0.027x + 0.132 respectively, where x refers to the entrance\exit doses and y refers to the entrance\exit OD and the attenuation coefficient of Perspex (phantom) has been derived correctly from the relationship between the phantom thickness and it's absorption coefficient which was 0.1670 cm-1. **(Mohammed A. Ali Omer, et al, 2015).**

Chapter three: Methodology

3.1. Materials:

- Polyvinyl Alcohol (PVA)

Polyvinyl alcohol powder supplied by TECHNO PHARMCHEM (Mol. wt = 85000 to 124000 g/mol Degree of hydrolysis 86-89%).

-Silver Nitrate Ag NO_3:

Silver Nitrate Chemical compound (powder) supplied by laboratory reagents and fine chemicals Ltd, sensitive to sun light in photographic films.

- Tools:

Distilled water, Volumetric Flask, Petri dish, Beakers, Volumetric flask, bottles

3.2. Experimental Apparatus:

3.2.1. X-ray Machine Unit:

- x-ray machine model PN563-55051-34 (Shimadzu) with filtration 1 mm AL, Max tube Voltage 150 KV, Frequency 50/60 Hz has been used for the irradiation of PVA/$AgNO_3$ films.

Figure (3.1) shows the x-ray machine unit of films irradiation.

3.2.2. UV- Visible Spectrophotometer:

UV-visible spectrophotometer Model V-650 UV/VIS/NIR was used to measure the absorption spectra. The instrument is specified by its resolution value of 0.1 nm and wavelength accuracy ± 0.30 nm (at a spectral bandwidth of 0.5 nm) in the UV/VIS region. Single monochromatic, UV/VIS region 1200 lines/mm plane grating, NIR region 300 lines/nm plane grating, Czerny-Turner mount, double beam type.

Figure (3.2) shows the UV- Visible spectrophotometer**.**

3.2.3. Optical Densitometer:

Optical Densitometer 331 battery operated, B/W transmission densitometer, operated voltage 4-6volt DC – SN 033174 has been used to measure the optical density of PVA/$AgNO_3$ films.

Figure (3.3) shows the optical densitometer.

3.2.4. X-ray Fluorescence:

X-ray Fluorescence Model CM/HM/ XRF-06 with serial number C13206 has been used to determine the dependence of intensity of AgLα characteristic X-Ray line on Ag concentration for PVA/AgNO3 nanocomposites.

Figure (3.4) shows the X-ray Fluorescence Instrument.

3.2.5: sensitive Balance:

Sensitive balance model ABT-220 – 4M has been used measure the weight of PVA and $AgNO_3$ to determine the concentrations (wt%) of PVA and $AgNO_3$ in the PVA/ $AgNO_3$ Films.

Figure (3.5) shows the sensitive Balance Instrument

3.2.6: Data Logger:

Data Logger model PRHTemp 2000 Was used to measure the temperature, Humidity and atmospheric pressure during the synthesis of PVA/AgNO3 films.

Figure (3.6) shows the data logger Instrument

3.2.7: Magnetic Stirrer:

Figure (3.7) shows the magnetic stirrer Instrument.

3.2.8: Micrometer:

Micrometer model 99MAA001M used to measure the thickness of PVA/$AgNO_3$ films.

Figure (3.8) shows the micrometer Instrument.

3.3. Methods:

The PVA Powder was supplied by TECHNO PHARMCHEM (Mol. wt = 85000 to 124000 g/mol Degree of hydrolysis 86-89%). The PVA/$AgNO_3$ Films were made through solvent casting technique with seven concentrations of $AgNO_3$/PVA percentage and that is, [C1=4%], [C2=5%], [C3=6%], [C4=10%], [C5=15%], [C6=20%], [C7=25%], by dissolving each concentration of PVA powder in 100 ml distilled water at room temperature on a beaker and The solutions were magnetically stirred at room temperature for 3 hours and then the PVA/$AgNO_3$ solutions poured in a petri-dish to form films by casting method in dark room. and left to dry at ambient temperature at least 2 days, the ambient condition was measured using data logger [Temperature = 22.7 C, Humidity = 29.3%, atmospheric pressure = 961 mBar] (**Muhammad Attique et al, 2014).**

Then films were peeled off in the petri-dish, cut into small films 2x2cm, loaded in sealed dark dental film envelope, The thickness of the films was measured using micrometer.

Figure (3.9) shows the tools used for PVA/AgNO3 synthesis.

Then the PVA/$AgNO_3$ films were irradiated with low x-ray doses in the range of diagnostic levels, [.15, 33, .59, .93, 1.34] mGy, the dose was controlled by the exposure factors Kvp and mAs, the range of exposure factors used between (40 – 120) Kvp and 10 mAs for x-ray machine.

The dose in mGy was measured using the equation:

$$ESD = OP \times \left(\frac{kV}{80}\right)^2 \times mAs \times \left(\frac{100}{FSD}\right)^2 \times BSF$$

Where:

(OP) is the output in mGy/ (mA) of the X-ray tube at 80 kV at a focus distance of 1 m normalized to 10 mA s, (kV) the tube potential,(mA) the product of the tube current (mA) and the exposure time(s), (FSD) the focus-to-skin distance (in cm). (BSF) the backscatter factor.

Figure (3.10) shows the irradiation of PVA/AgNO3 to low x-ray doses.

The PVA/AgNO3 films analysis using XRF to determine the dependence of intensity of AgLα characteristic X-Ray line on Ag concentration for PVA/AgNO3 nanocomposites then the PVA/AgNO3 films were analyzed using UV-visible spectrophotometer to measure the absorption spectra then the optical density of PVA/AgNO3 films was measured using optical densitometer, The data will analyze with Excel program to assess the correlation between x-ray doses and optical density, optical density and concentration. Also Lab Origin program were used to view the absorption spectra of PVA/AgNO3 Films irradiated with different doses.

Chapter Four: Result

The following chapter will the experimental result of prepared PVA\$AgNO_3$ composites films and their characterization after irradiation with doses in the diagnostic range.

4.1 Color formation change:

Figure (4.1) shows the change in PVA/AgNO3 films color intensity due to irradiation with low x-ray doses.

4.2. X-ray Fluorescence Measurement:

X-ray Fluorescence was used to validate that the intensity of AgLα characteristic X-Ray line depends on the Ag concentration in the PVA/AgNO3 films.

Table 4.1 shows the intensity of AgLα characteristic X-Ray line for PVA/AgNO3 films irradiated with doses [0.15, 0.33, 0.59, 0.93, 1.34 mGy]

AgNO3 Concentration	intensity of AgLα For films irradiated with 0.15 mGy	intensity of AgLα For films irradiated with 0.33 mGy	intensity of AgLα For films irradiated with 0.59 mGy	intensity of AgLα For films irradiated with 0.93 mGy	intensity of AgLα For films irradiated with 1.34 mGy
4%	940.8	935.2	932.8	932.2	921.9
5%	948.0	942.1	935.8	940.8	933.5
6%	953.4	952.7	943.1	945.7	943.0
10%	960.3	958.3	952.1	956.8	948.0
15%	972.6	963.1	959.2	959.7	953.0
20%	974.3	971.3	960.3	964.0	958.0
25%	977.4	974.3	972.6	977.0	963.0

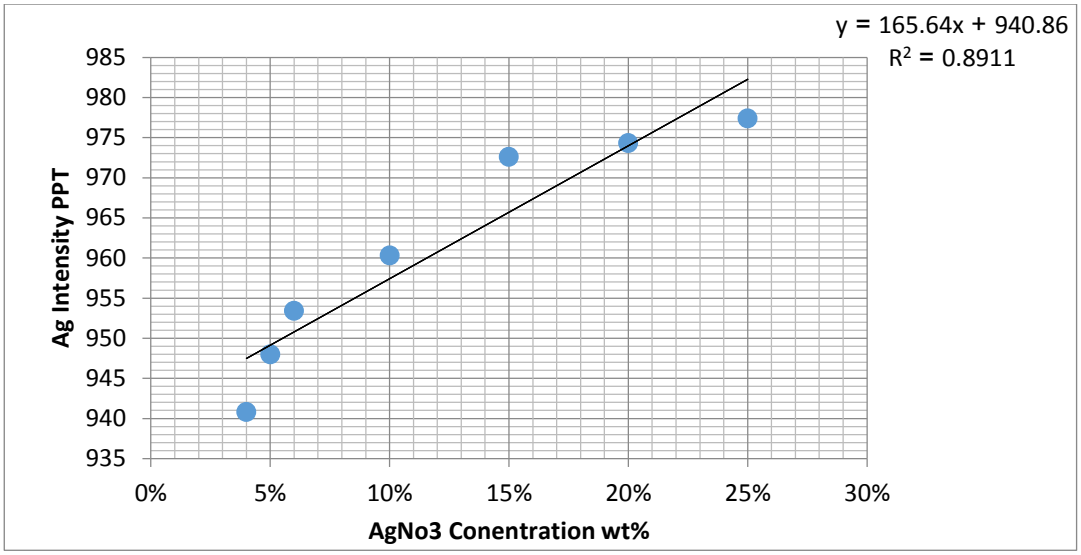

Figure [4.2]: Dependence of intensity of AgL$_\alpha$ characteristic X-Ray line on Ag concentration for PVA/$AgNO_3$ films irradiated with 0.15 mGy.

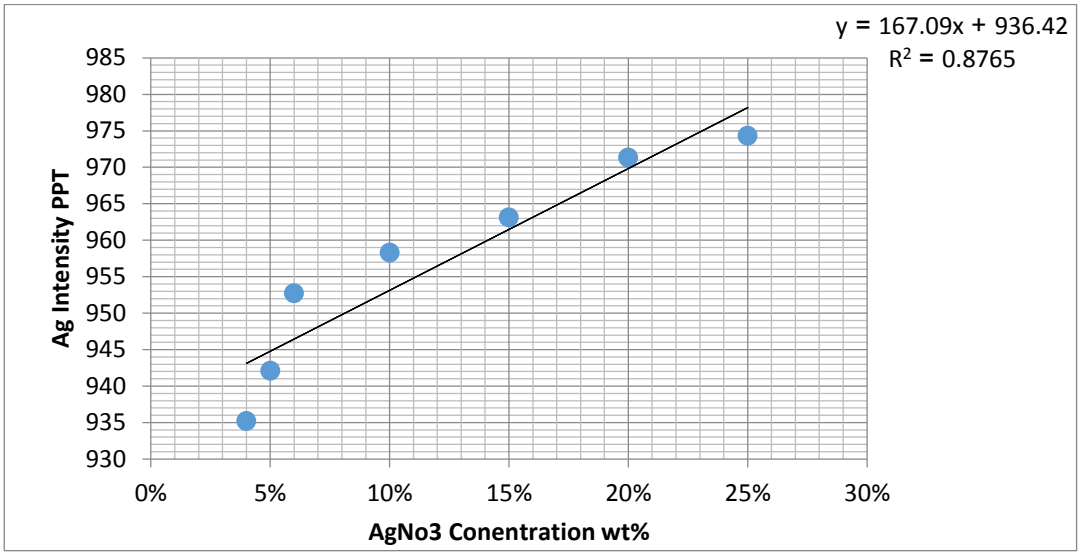

Figure [4.3]: Dependence of intensity of AgL$_\alpha$ characteristic X-Ray line on Ag concentration for PVA/$AgNO_3$ films irradiated with 0.33 mGy.

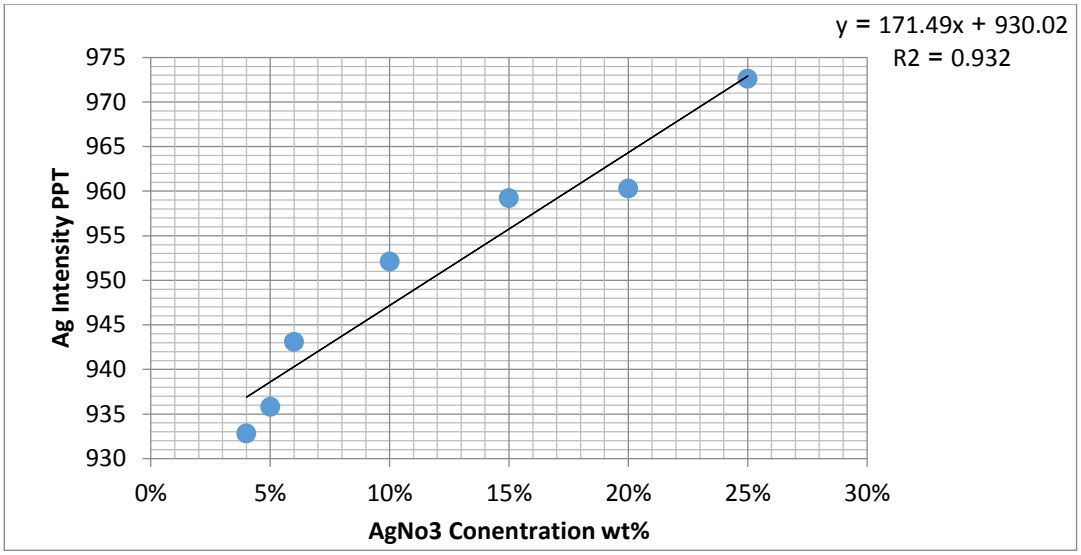

Figure [4.4]: Dependence of intensity of AgL$_\alpha$ characteristic X-Ray line on Ag concentration for PVA/$AgNO_3$ films irradiated with 0.59 mGy.

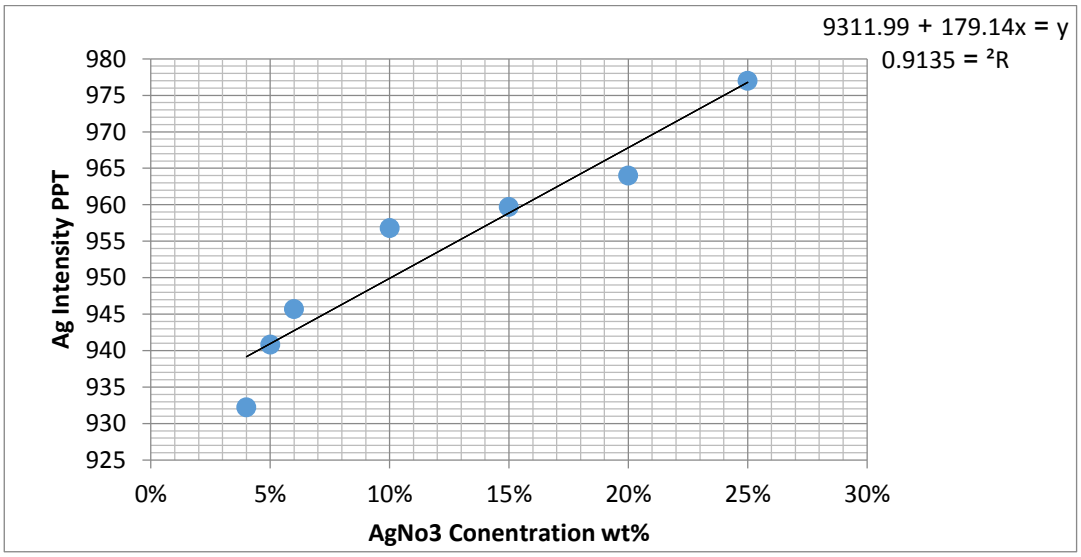

Figure [4.5]: Dependence of intensity of AgL$_\alpha$ characteristic X-Ray line on Ag concentration for PVA/$AgNO_3$ films irradiated with 0.93 mGy.

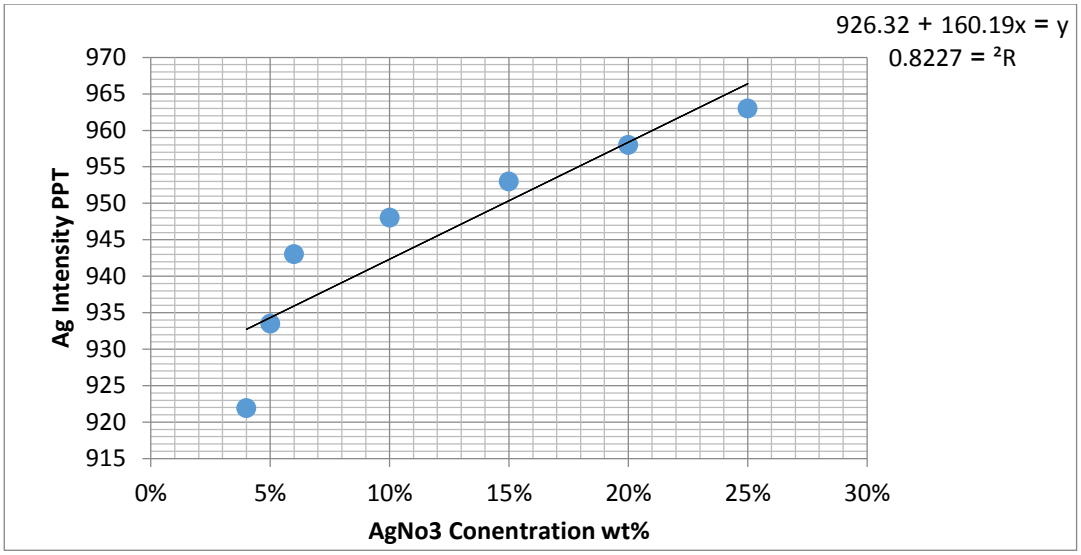

Figure [4.6]: Dependence of intensity of AgL_{α} characteristic X-Ray line on Ag concentration for PVA/$AgNO_3$ films irradiated with 1.34 mGy.

4.3. Optical Densitometer Measurement:

Table 4.2 shows the optical density measurement for PVA/AgNO3 films with different concentration of $AgNO_3$ irradiated with doses [0.15, 0.33, 0.59, 0.93, 1.34 mGy]

AgNO3 Concentration	Optical density of PVA/AgNO3 films irradiated with 0.15 mGy	Optical density of PVA/AgNO3 films irradiated with 0.33 mGy	Optical density of PVA/AgNO3 films irradiated with 0.59 mGy	Optical density of PVA/AgNO3 films irradiated with 0.93 mGy	Optical density of PVA/AgNO3 films irradiated with 1.34 mGy
4%	0.27	0.37	0.42	0.43	0.46
5%	0.28	0.38	0.43	0.44	0.47
6%	0.30	0.39	0.44	0.45	0.47
10%	0.38	0.41	0.45	0.46	0.48
15%	0.57	0.63	0.68	0.72	0.76
20%	0.62	0.67	0.72	0.83	0.95
25%	0.77	0.84	0.87	0.90	0.98

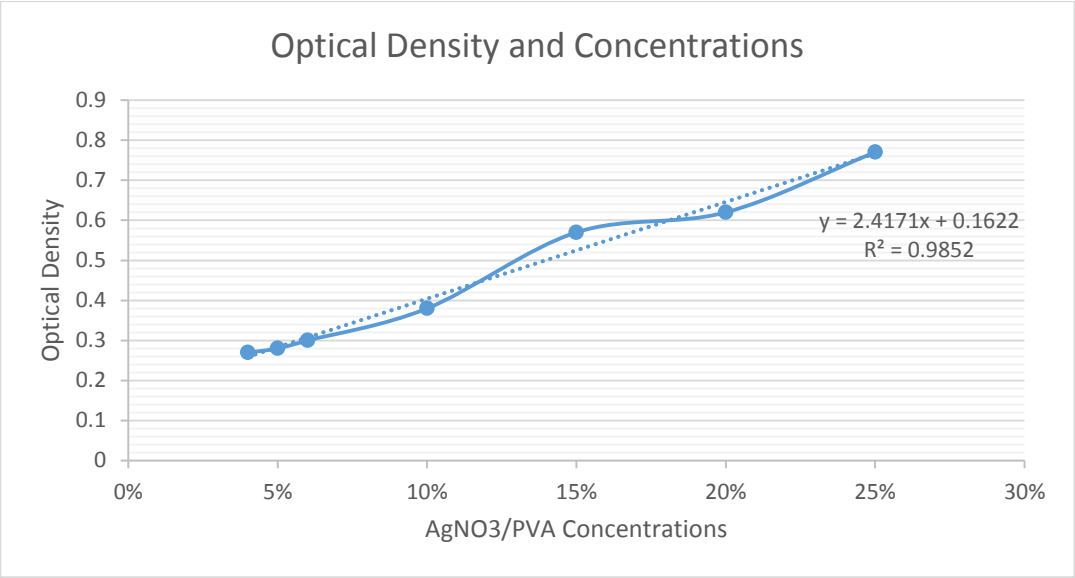

Figure [4.7]: The Correlation between AgNO3/PVA concentrations and optical density.

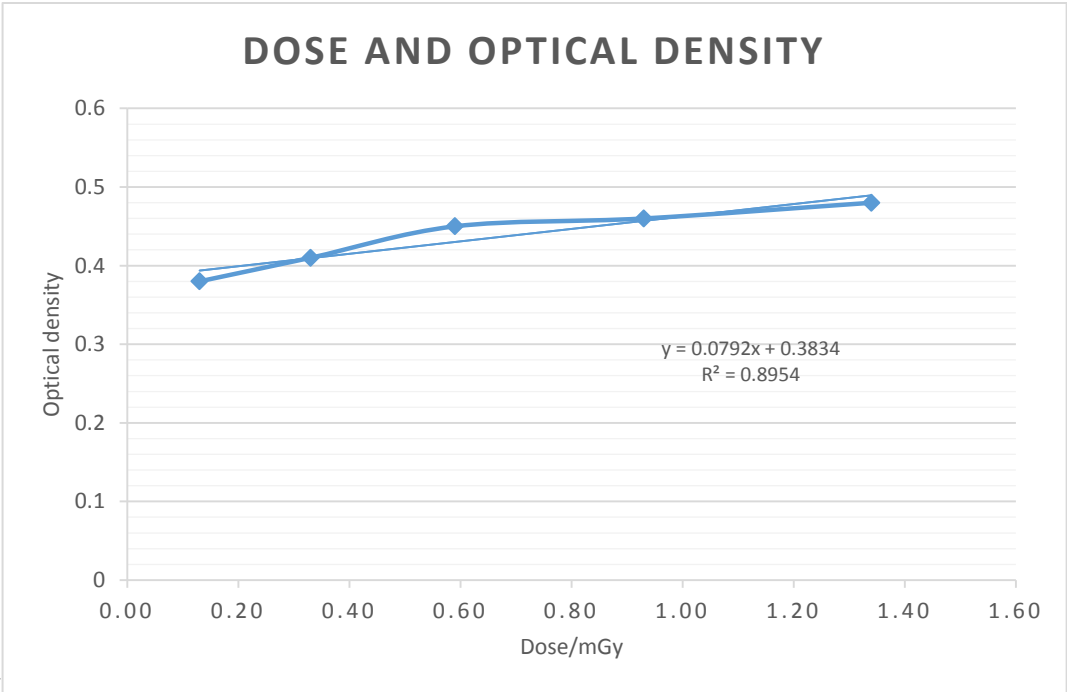

Figure [4.8]: The Correlation between Radiation Dose and optical density.

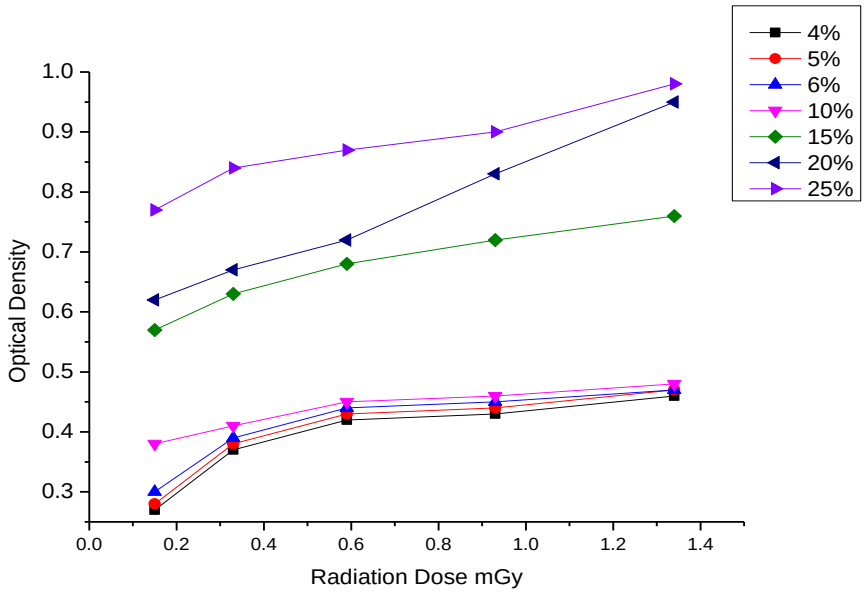

Figure [4.9]: The effect of $AgNO_3$ Concentrations and Dose on the optical density of PVA/$AgNO_3$ films.

4.4. UV- Visible Spectroscopy Measurement:

The absorption spectra of irradiated PVA/$AgNO_3$ films were measured in the wavelength range of 200-800nm, used un irradiated PVA/$AgNO_3$ films as reference. The absorption spectra of PVA/$AgNO_3$ films were recorded at different x-ray doses.

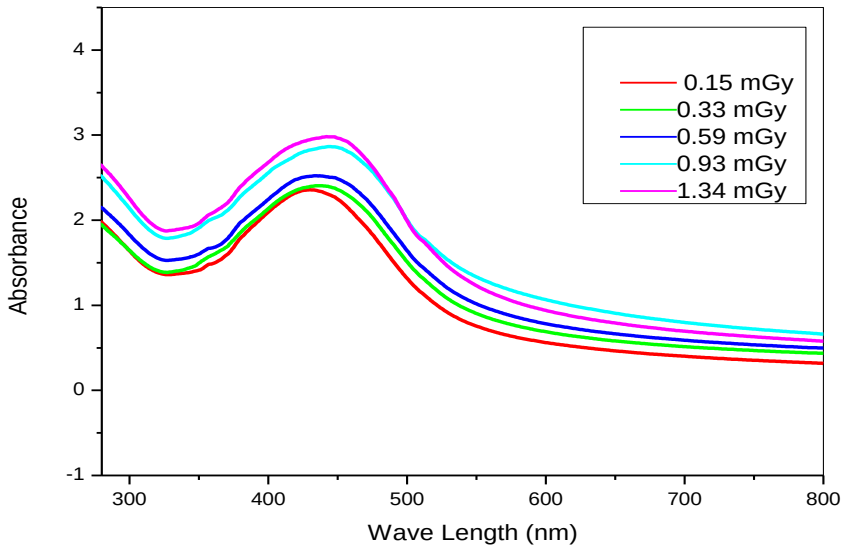

Figure [4.10]: the UV spectrum of PVA/AgNO3 films with concentrations of 4% irradiated with different doses.

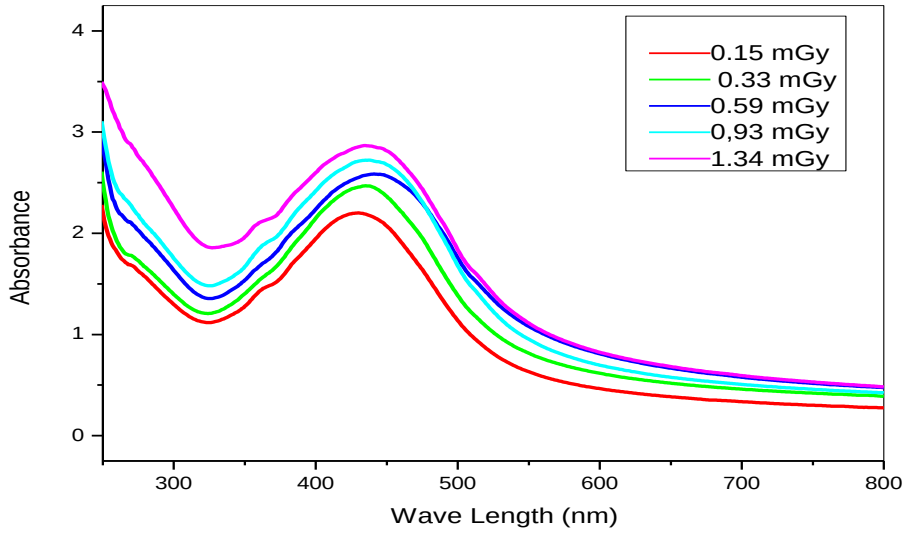

Figure [4.11] the UV spectrum of PVA/AgNO3 films with concentrations of 5% irradiated with different doses.

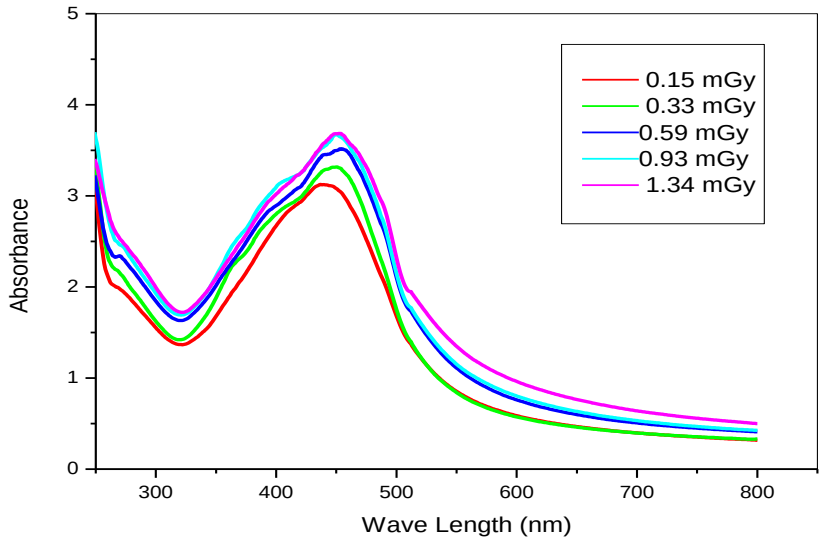

Figure [4.12] the UV spectrum of PVA/AgNO3 films with concentrations of 6% irradiated with different doses.

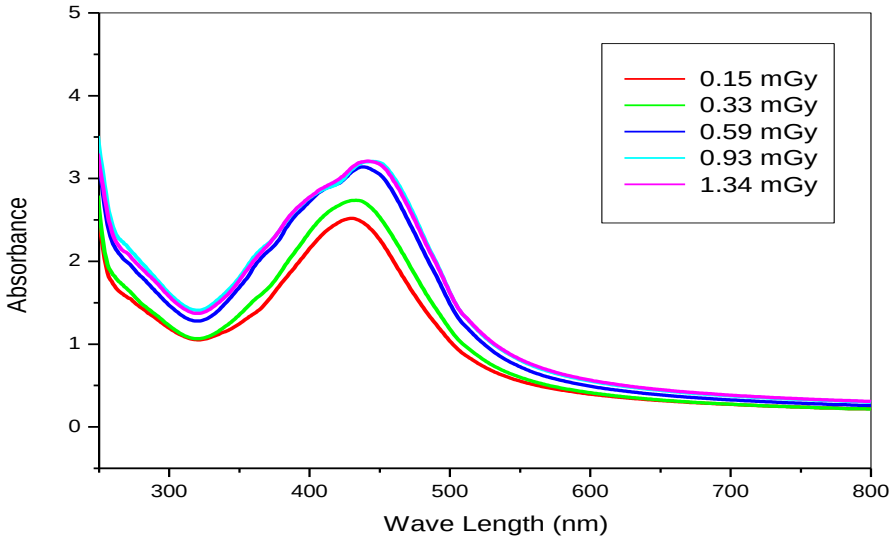

Figure [4.13] the UV spectrum of PVA/AgNO3 films with concentrations of 10% irradiated with different doses.

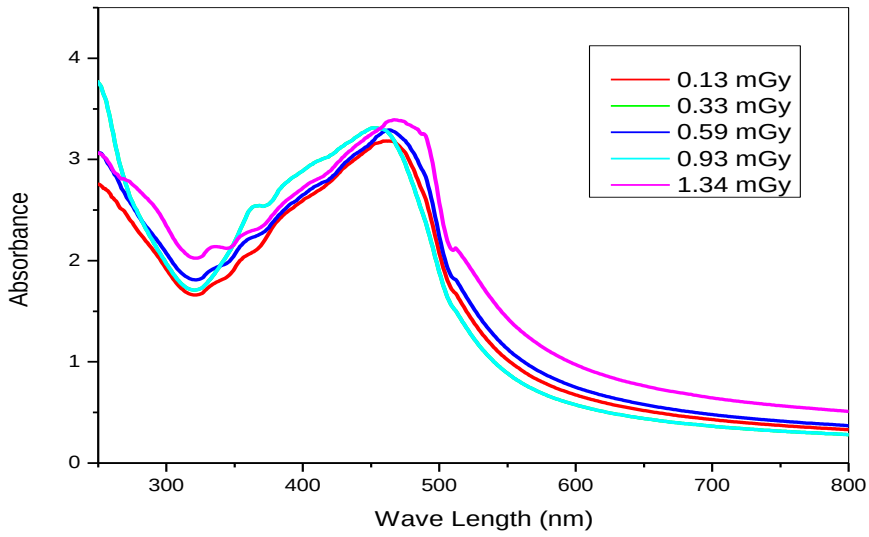

Figure [4.14] the UV spectrum of PVA/AgNO3 films with concentrations of 15% irradiated with different doses.

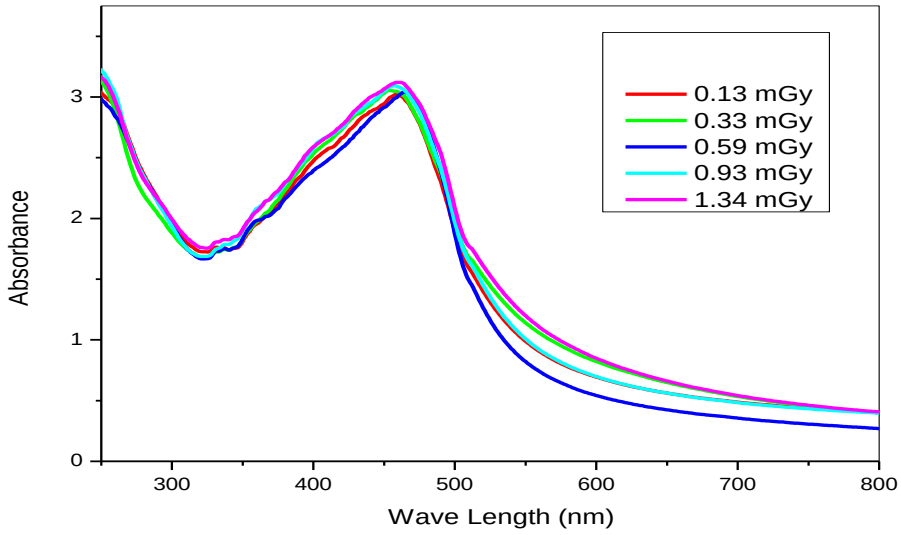

Figure [4.15] the UV spectrum of PVA/AgNO3 films with concentrations of 20% irradiated with different doses.

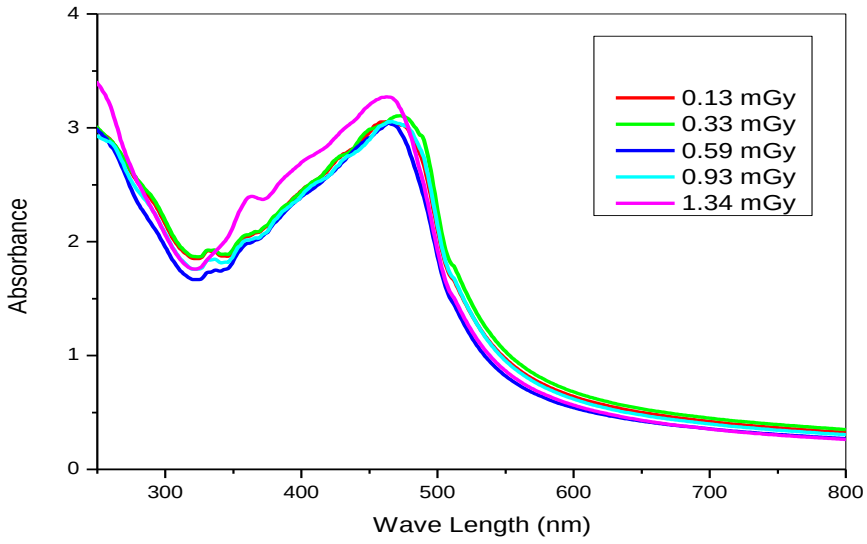

Figure [4.16]: the UV spectrum of PVA/AgNO3 films with concentrations of 25% irradiated with different doses.

Table 4.3 shows the Specific Absorbance measurement of PVA/AgNO3 films with different concentration of $AgNO_3$ irradiated with doses [0.15, 0.33, 0.59, 0.93, 1.34 mGy]

AgNO3 Concentration	Specific Absorbance of PVA/AgNO3 films irradiated with 0.15 mGy	Specific Absorbance of PVA/AgNO3 films irradiated with 0.33 mGy	Specific Absorbance of PVA/AgNO3 films irradiated with 0.59 mGy	Specific Absorbance of PVA/AgNO3 films irradiated with 0.93 mGy	Specific Absorbance of PVA/AgNO3 films irradiated with 1.34 mGy
4%	2.38	2.43	2.55	2.89	3.03
5%	2.21	2.49	2.60	2.75	2.89
6%	3.18	3.36	3.64	3.77	3.78
10%	2.53	2.78	3.17	3.27	3.27
15%	3.26	3.34	3.36	3.34	3.48
20%	3.05	3.10	3.10	3.14	3.17
25%	3.13	3.17	3.10	3.13	3.36

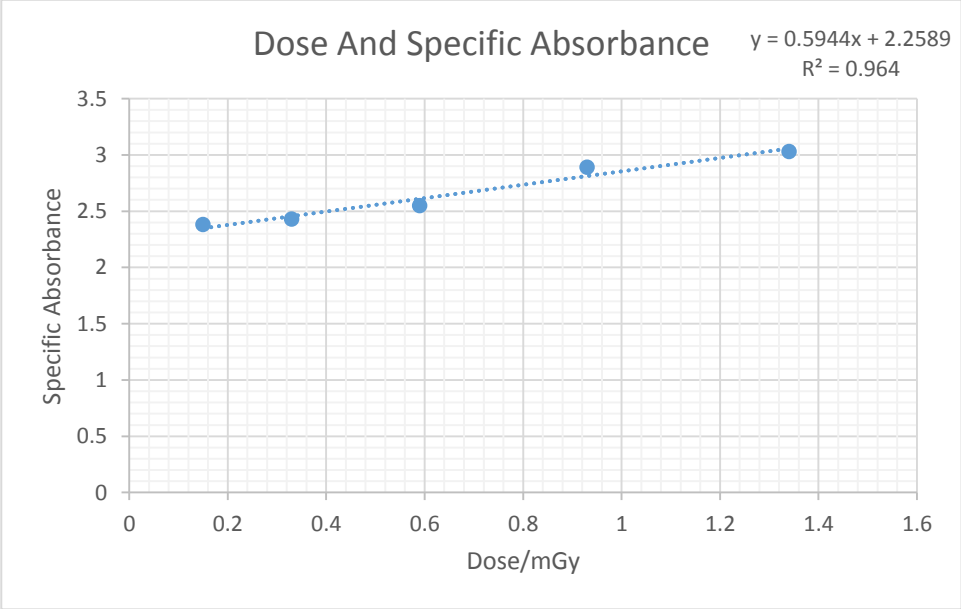

Figure [4.17]: The Correlation between dose/mGy and specific absorbance for PVA/AgNO3 films of 4% concentration irradiated with different doses.

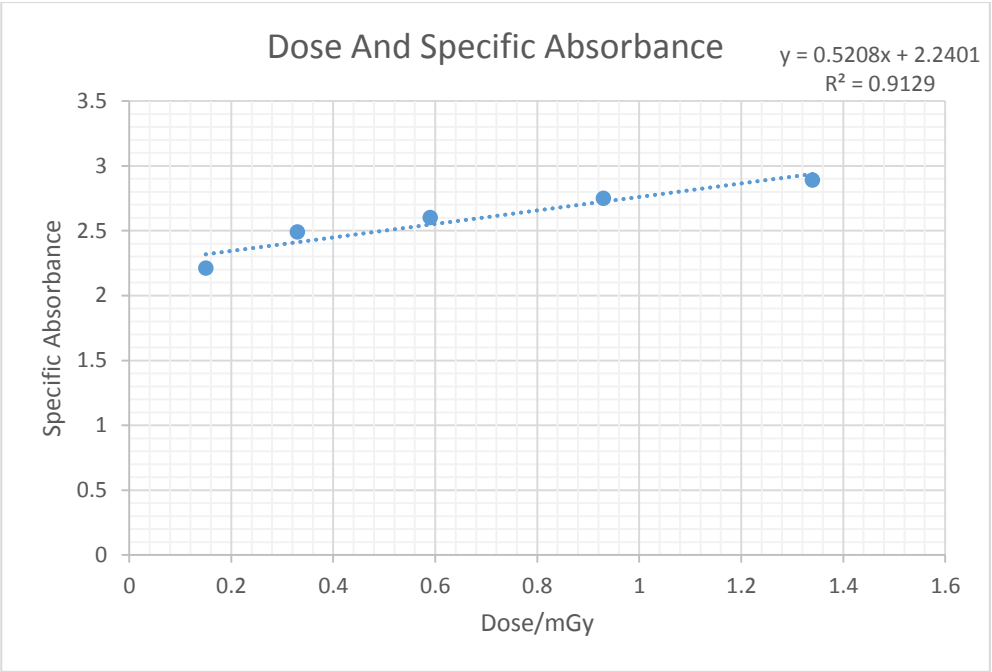

Figure [4.18]: The Correlation between dose/mGy and specific absorbance for PVA/AgNO3 films of 5% concentration irradiated with different doses.

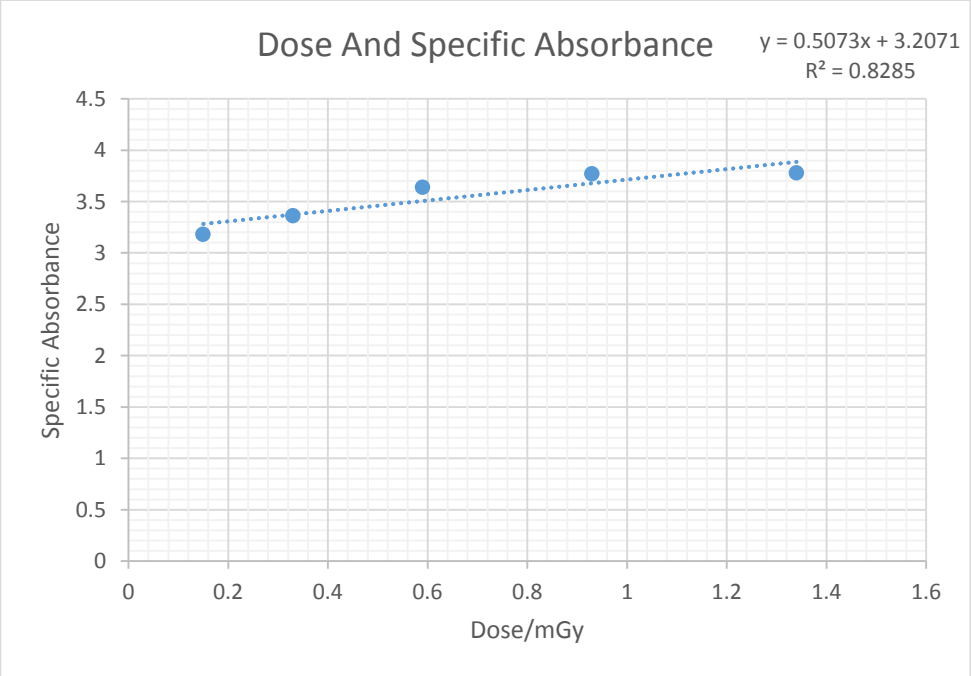

Figure [4.19]: The Correlation between dose/mGy and specific absorbance for PVA/AgNO3 films of 6% concentration irradiated with different doses.

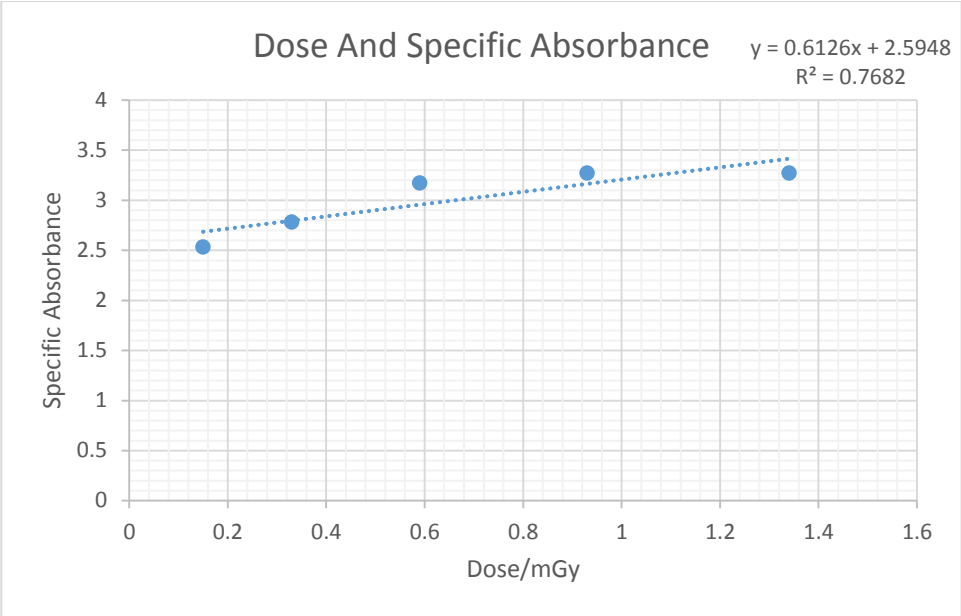

Figure [4.20]: The Correlation between dose/mGy and specific absorbance for PVA/AgNO3 films of 10% concentration irradiated with different doses.

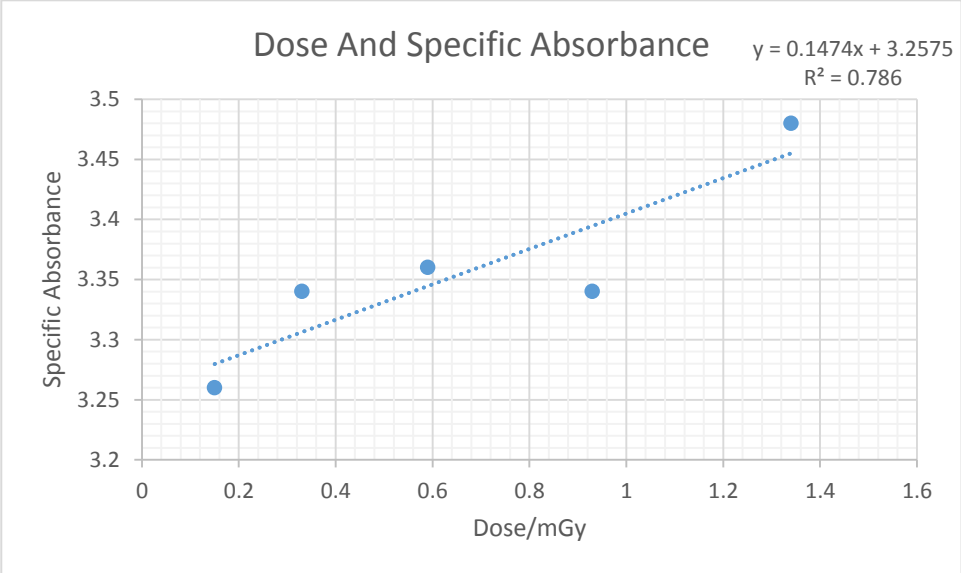

Figure [4.21]: The Correlation between dose/mGy and specific absorbance for PVA/AgNO3 films of 15% concentration irradiated with different doses.

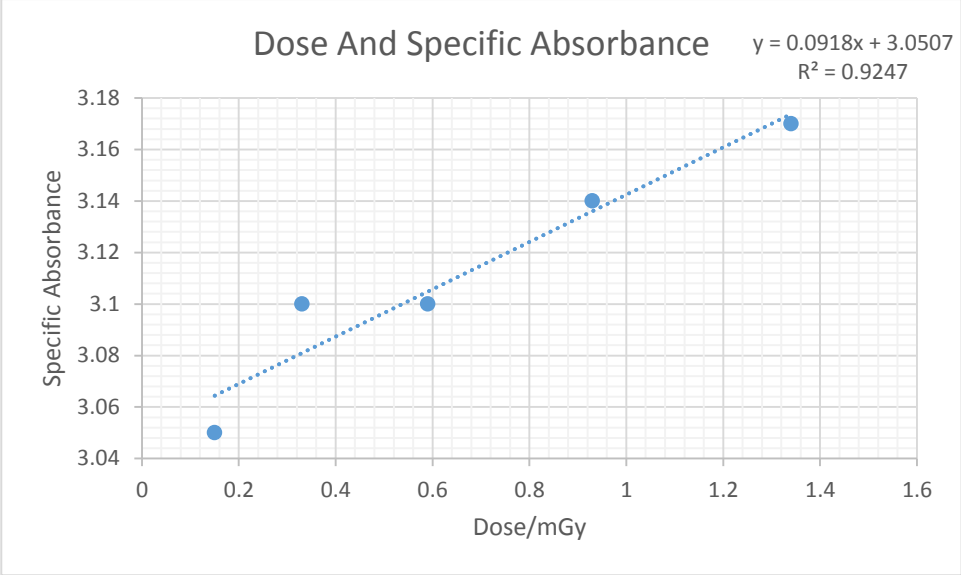

Figure [4.22]: The Correlation between dose/mGy and specific absorbance for PVA/AgNO3 films of 20% concentration irradiated with different doses.

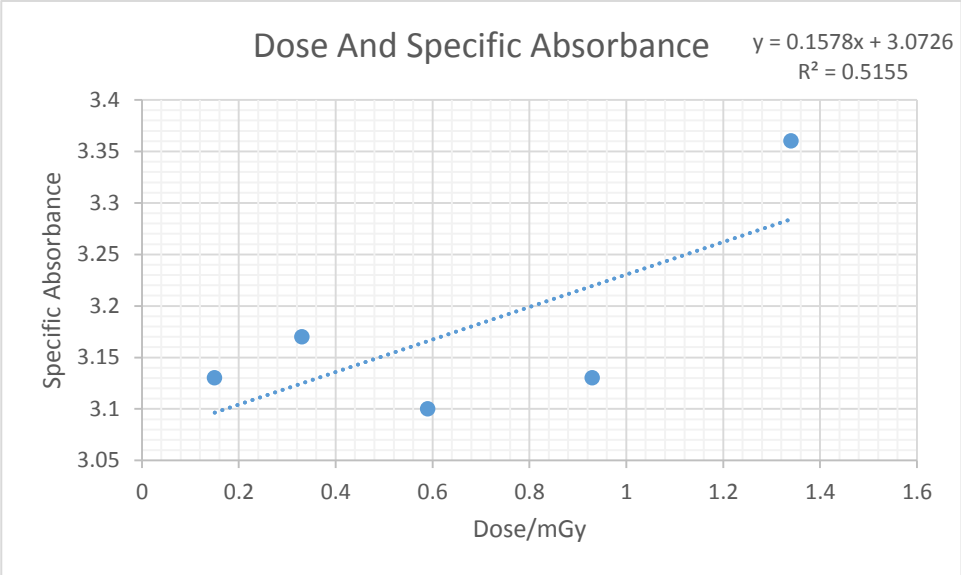

Figure [4.23]: The Correlation between dose/mGy and specific absorbance for PVA/AgNO3 films of 25% concentration irradiated with different doses.

Table 4.4 shows the thickness of PVA/AgNO3 films measured using micrometer. Average = .11 mm = 110 μm

AgNO3 Concentration	Thickness/mm of PVA/AgNO3 films irradiated with 0.15 mGy	Thickness/mm of PVA/AgNO3 films irradiated with 0.33 mGy	Thickness/mm of PVA/AgNO3 films irradiated with 0.59 mGy	Thickness/mm of PVA/AgNO3 films irradiated with 0.93 mGy	Thickness/mm of PVA/AgNO3 films irradiated with 1.34 mGy
4%	0.1	0.11	0.09	0.12	0.08
5%	0.09	0.12	0.09	0.11	0.08
6%	0.12	0.11	0.10	0.10	0.11
10%	0.12	0.13	0.11	0.12	0.13
15%	0.13	0.12	0.14	0.13	0.12
20%	0.09	0.09	0.10	0.09	0.08
25%	0.11	0.14	0.13	0.11	0.12

Table 4.5 shows the Absorption Coefficient measurement of PVA/AgNO3 films with different concentration of $AgNO_3$ irradiated with doses [0.15, 0.33, 0.59, 0.93, 1.34 mGy]

AgNO3 Concentration	Absorption Coefficient of PVA/AgNO3 films irradiated with 0.15 mGy	Absorption Coefficient of PVA/AgNO3 films irradiated with 0.33 mGy	Absorption Coefficient of PVA/AgNO3 films irradiated with 0.59 mGy	Absorption Coefficient of PVA/AgNO3 films irradiated with 0.93 mGy	Absorption Coefficient of PVA/AgNO3 films irradiated with 1.34 mGy
4%	0.049	0.051	0.053	0.061	0.063
5%	0.046	0.052	0.054	0.058	0.061
6%	0.067	0.070	0.076	0.079	0.079
10%	0.053	0.058	0.066	0.068	0.068
15%	0.068	0.069	0.070	0.069	0.073
20%	0.063	0.065	0.065	0.066	0.066
25%	0.065	0.066	0.065	0.065	0.070

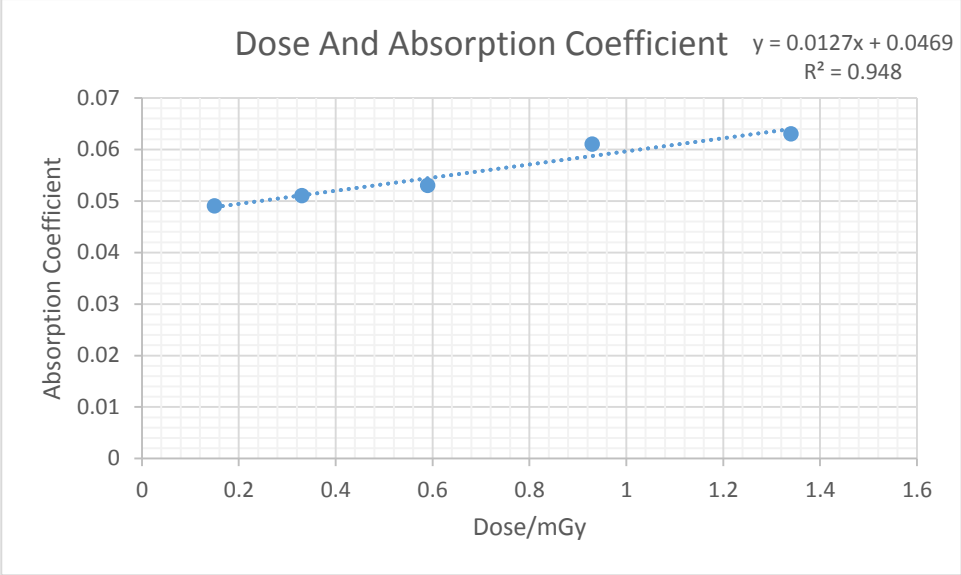

Figure [4.24]: The Correlation between dose/mGy and Absorption Coefficient for PVA/AgNO3 films of 4% concentration irradiated with different doses.

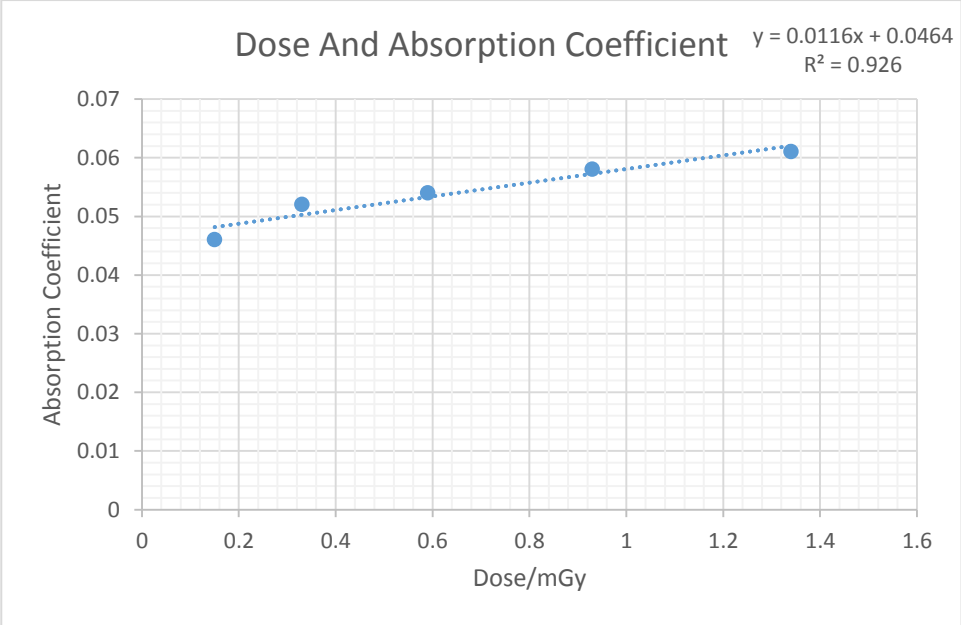

Figure [4.25]: The Correlation between dose/mGy and Absorption Coefficient for PVA/AgNO3 films of 5% concentration irradiated with different doses.

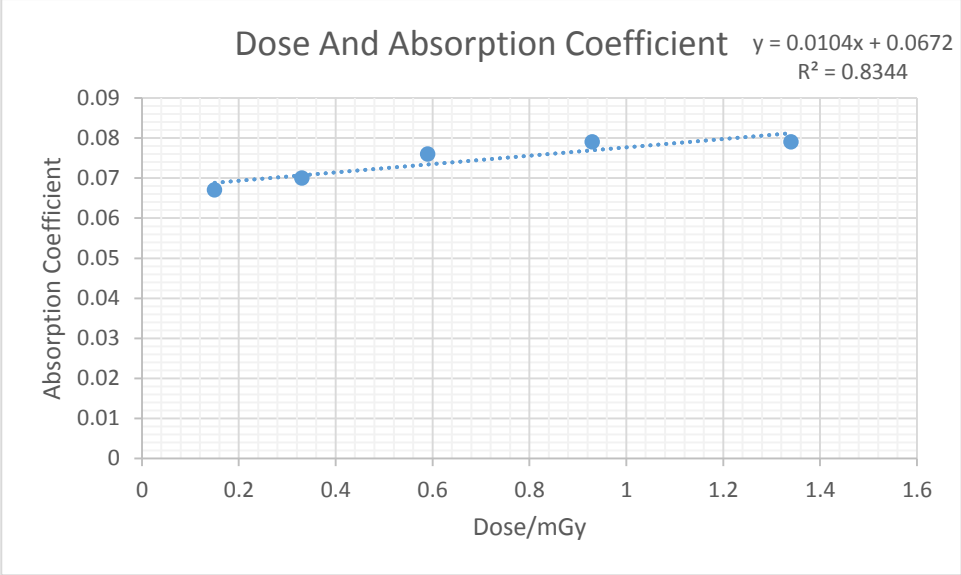

Figure [4.26]: The Correlation between dose/mGy and Absorption Coefficient for PVA/AgNO3 films of 6% concentration irradiated with different doses.

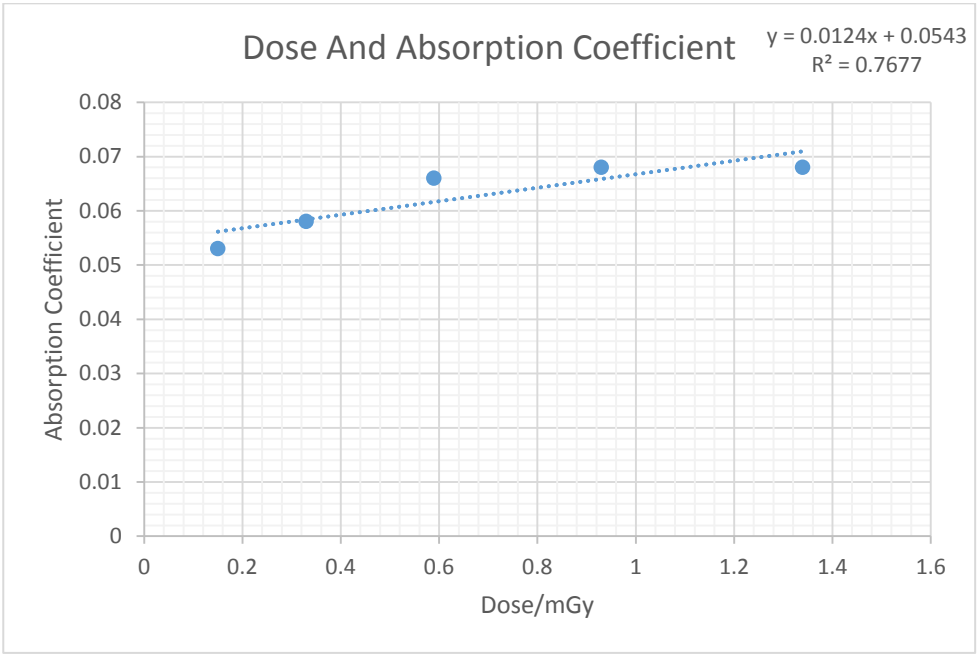

Figure [4.27]: The Correlation between dose/mGy and Absorption Coefficient for PVA/AgNO3 films of 10% concentration irradiated with different doses.

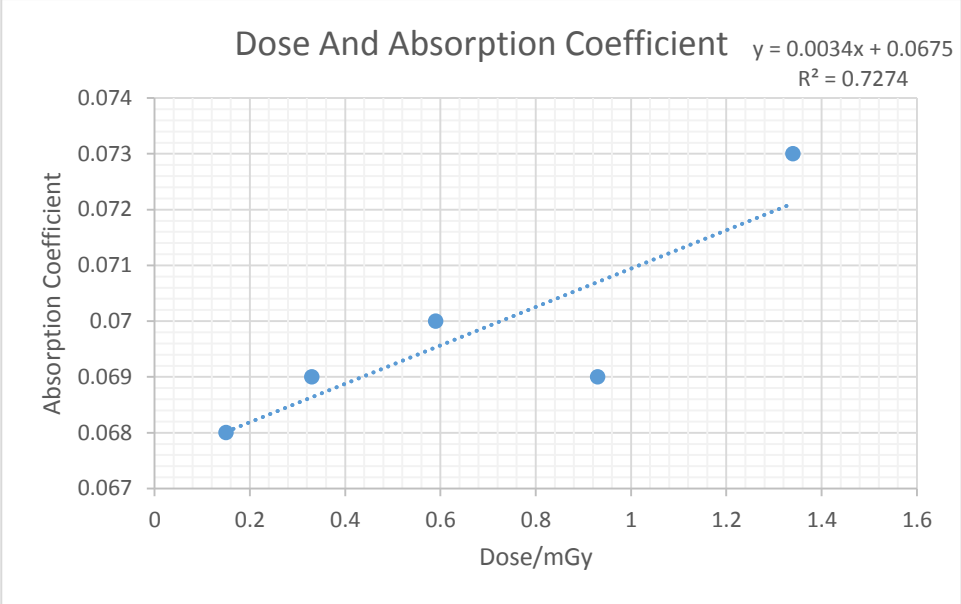

Figure [4.28]: The Correlation between dose/mGy and Absorption Coefficient for PVA/AgNO3 films of 15% concentration irradiated with different doses.

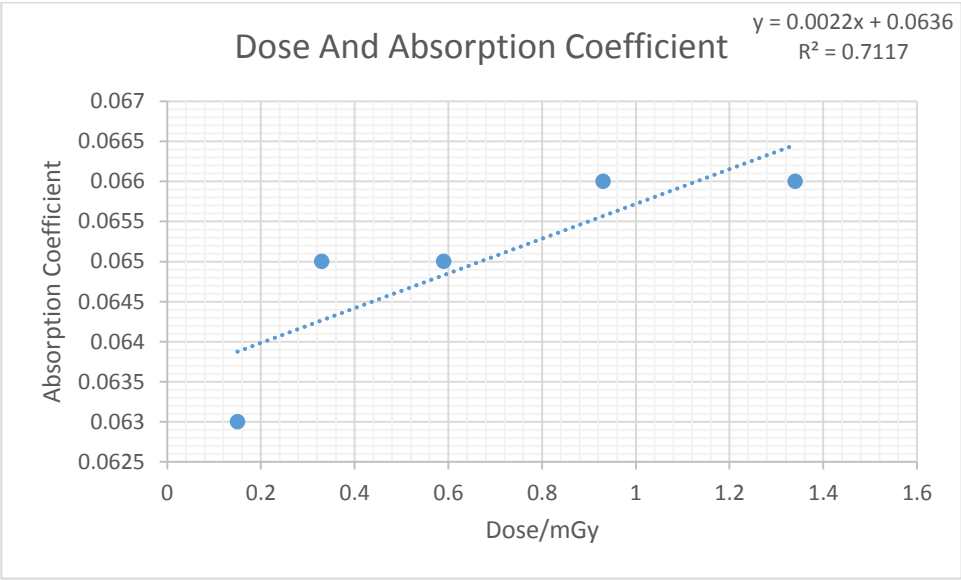

Figure [4.29]: The Correlation between dose/mGy and Absorption Coefficient for PVA/AgNO3 films of 20% concentration irradiated with different doses.

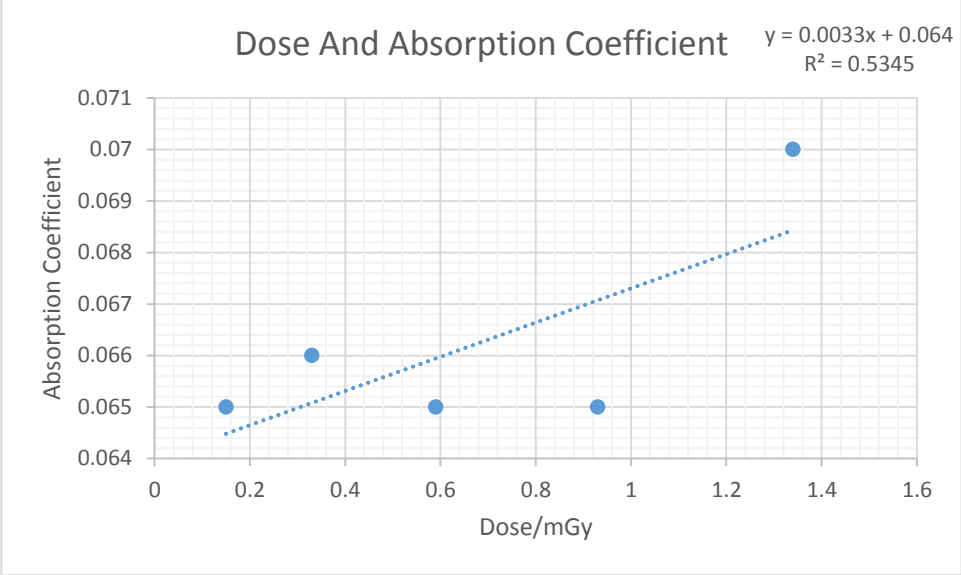

Figure [4.30]: The Correlation between dose/mGy and Absorption Coefficient for PVA/AgNO3 films of 25% concentration irradiated with different doses.

Before irradiation x-ray machine was calibrated to check that the kilo voltage and milliampere second is within the tolerance using KV meter, KVp measurement for the x-ray machine machine is within the tolerance limit (± 5%), Milliampere second measurement for the x-ray machine is within the tolerance limit (± 10%) except at 250 mAs.

Table (4.6) show the setting and measured Kvp and mAs for x-ray machine.

kilo voltage			Milliampere second		
Setting	Measured	Accuracy %	Setting	Measured	Accuracy %
85	85.1	0.12	200	186.1	6.95
80	79.6	0.50	40	40.7	1.75
75	74.2	1.07	160	158.5	0.94
70	68.4	2.29	64	65.4	2.19
65	64	1.54	50	51.3	2.60
60	61.3	2.17	100	100.9	0.90
55	53	3.64	250	216.8	13.28
50	48.7	2.60	80	81.5	1.88
45	44.8	0.44	125	127.6	2.08

4.5. Discussion:

In the present study the PVA/$AgNO_3$ films with different concentrations of Ag NO_3 (4, 5, 6, 10, 15, 20 and 25) wt% were prepared by casting method and the reduction of Ag+ ions in PVA/$AgNO_3$ films was done by using x-ray irradiation with different x-ray doses of (0.15, 0.33, 0.59, 0.93, 1.34) mGy.

Figure (4.1) shows the PVA/$AgNO_3$ films undergoing color change after irradiated with x-ray doses of (0.15, 0.33, 0.59, 0.93, 1.34) mGy. The color intensity was increase with increasing x-ray doses indication that the color change is largely dependent on the proportion of the red and yellow color components, the color changed from gray (un-irradiated film) then to color combination of light yellow, golden, brown and dark brown following increasing intensity with increasing x-ray doses. Such color change has been reported by (Omer M. et al, 2011), (Muhammad Attique. et al, 2014), (Susilawati. et al, 2009), (Shaheen Akhtar. et al, 2013), (Iskandar. et al, 2013).

X-ray Fluorescence analysis was done to validate that the intensity of AgLα characteristic X-Ray line depends on the Ag concentration in the PVA/AgNO3 films.

Figure [4.2] shows strong Dependence of intensity of AgLα characteristic X-Ray line on Ag concentration for PVA/AgNO3 films irradiated with 0.15 mGy with correlation coefficient $\mathbf{R^2 = 0.8911}$ and the correlation equation **Y=165.64X+940.86**, Figure [4.3] shows strong Dependence of intensity of AgLα characteristic X-Ray line on Ag concentration for PVA/AgNO3 films irradiated with 0.33 mGy with correlation coefficient $\mathbf{R^2 = 0.8765}$ and the correlation equation **Y= 167.09X+936.42**, Figure [4.4] shows strong Dependence of intensity of AgLα characteristic X-Ray line on Ag concentration for PVA/AgNO3 films irradiated with 0.59 mGy with correlation coefficient $\mathbf{R^2 = 0.8765}$ and the correlation equation **Y= 167.09X+936.42**, Figure [4.5] shows strong Dependence of intensity of AgLα characteristic X-Ray line on Ag concentration for PVA/AgNO3 films

irradiated with 0.93 mGy with correlation coefficient $\mathbf{R^2 = 0.9135}$ and the correlation equation **Y= 179.14X+931.99**, Figure [4.6] shows strong Dependence of intensity of AgLα characteristic X-Ray line on Ag concentration for PVA/AgNO3 films irradiated with 1.34 mGy with correlation coefficient $\mathbf{R^2 = 0.8227}$ and the correlation equation **Y= 160.19X+926.32**

Optical Densitometer analysis was done to evaluate the sensitivity of PVA/$AgNO_3$ composites films to low x-ray doses and the effect of $AgNO_3$ concentrations in the PVA/$AgNO_3$ composites films. figure [4.7] showed positive correlation between $AgNO_3$ concentrations and optical density of PVA/$AgNO_3$ composites films with correlation coefficient $\mathbf{R^2 = 0.9852}$ and the correlation equation **Y= 0.1622X+2.4171,** figure [4.8] showed positive correlation between irradiated x-ray Doses and optical density of PVA/$AgNO_3$ composites films with correlation coefficient $\mathbf{R^2 = 0.8954}$ and the correlation equation **Y= 0.3834X+0.0792**, figure [4.9] showed that for all PVA/$AgNO_3$ prepared with different concentrations [4, 5, 6, 10, 15, 20 and 25] wt% irradiated with different x-ray doses [0.15, 0.33, 0.59, 0.93, 1.34] mGy the optical density of PVA/$AgNO_3$ composites films increase linearly with x-ray doses and $AgNO_3$ concentration, same study has been reported by **(Mohammed A. Ali Omer, et al, 2015)** and they found that Also there is a linear proportional and significant (R2 = 0.9) relationship between the entrance\exit doses measured by TLD and the relative OD at both sides of the phantom which could be fitted in the following equation: y = 0.035x + 0.159 and y = 0.027x + 0.132 respectively, where x refers to the entrance\exit doses and y refers to the entrance\exit OD, this equation will be used to correct PVA/$AgNO_3$ films reading to TLD.

The absorption spectra of irradiated PVA/$AgNO_3$ films were measured in the wavelength range of 200-800nm, used un irradiated PVA/$AgNO_3$ films as reference. The absorption spectra of PVA/$AgNO_3$ films were recorded at different x-ray doses. figure [4.10] shows

the UV-spectrum for PVA/$AgNO_3$ films prepared with (4) wt% of $AgNO_3$ irradiated with x-ray doses [0.15, 0.33, 0.59, 0.93, 1.34] mGy, it is showed that all irradiated films has absorption peak at [430, 435, 434, 445, 442] nm respectively, the absorption peak increased with increasing x-ray doses. figure [4.11] shows the UV-spectrum for PVA/$AgNO_3$ films prepared with (5) wt% of $AgNO_3$ irradiated with x-ray doses [0.15, 0.33, 0.59, 0.93, 1.34] mGy, it is showed that all irradiated films has absorption peak at [430, 435, 441, 438, 435] nm respectively, the absorption peak increased with increasing x-ray doses. figure [4.12] shows the UV-spectrum for PVA/$AgNO_3$ films prepared with (6) wt% of $AgNO_3$ irradiated with x-ray doses [0.15, 0.33, 0.59, 0.93, 1.34] mGy, it is showed that all irradiated films has absorption peak at [437, 448, 455, 450, 454] nm respectively, the absorption peak increased with increasing x-ray doses. figure [4.13] shows the UV-spectrum for PVA/$AgNO_3$ films prepared with (10) wt% of $AgNO_3$ irradiated with x-ray doses [0.15, 0.33, 0.59, 0.93, 1.34] mGy, it is showed that all irradiated films has absorption peak at [430, 433, 439, 445, 442] nm respectively, the absorption peak increased with increasing x-ray doses. figure [4.14] shows the UV-spectrum for PVA/$AgNO_3$ films prepared with (15) wt% of $AgNO_3$ irradiated with x-ray doses [0.15, 0.33, 0.59, 0.93, 1.34] mGy, it is showed that all irradiated films has absorption peak at [459, 454, 464, 454, 467] nm respectively, the absorption peak increased with increasing x-ray doses. figure [4.15] shows the UV-spectrum for PVA/$AgNO_3$ films prepared with (20) wt% of $AgNO_3$ irradiated with x-ray doses [0.15, 0.33, 0.59, 0.93, 1.34] mGy, it is showed that all irradiated films has absorption peak at [459, 453, 464, 457, 460] nm respectively, the absorption peak increased with increasing x-ray doses. figure [4.16] shows the UV-spectrum for PVA/$AgNO_3$ films prepared with (25) wt% of $AgNO_3$ irradiated with x-ray doses [0.15, 0.33, 0.59, 0.93, 1.34] mGy, it is showed that all irradiated films has absorption peak at [464, 473, 464, 464, 462] nm respectively, the absorption peak

increased with increasing x-ray doses, same study with different absorption peak has been done by (Omer M. et al, 2011), (Muhammad Attique. et al, 2014), (Susilawati. et al, 2009), (AbdonMohd. et al, 2014), (Shaheen Akhtar. et al, 2013), (Iskandar. et al, 2013). Specific Absorbance was measured from absorption spectrum of all PVA/AgNO3 films with different concentration of $AgNO_3$ [4, 5, 6, 10, 15, 20, 25] wt% each film irradiated with x-ray doses [0.15, 0.33, 0.59, 0.93, 1.34] mGy. Figures [4.17], [4.18], [4.19], [4.20], [4.21], [4.22] and [4.23] showed strong Correlation between x-ray dose/mGy and specific absorbance for PVA/AgNO3 films of [4], [5], [6], [10], [15], [20], [25] wt% concentration, the correlation coefficient was [0.964], [0.9129], [0.8285], [0.7682], [0.786], [0.9247], [0.5155] respectively. Absorption coefficient was measured from Specific Absorbance of all PVA/AgNO3 films with different concentration of $AgNO_3$ [4, 5, 6, 10, 15, 20, 25] wt% each film irradiated with x-ray doses [0.15, 0.33, 0.59, 0.93, 1.34] mGy. Figures [4.24], [4.25], [4.26], [4.27], [4.28], [4.29] and [4.30] showed strong Correlation between x-ray dose/mGy and Absorption coefficient for PVA/AgNO3 films of [4], [5], [6], [10], [15], [20], [25] wt% concentration, the correlation coefficient was [0.948], [0.926], [0.8344], [0.7677], [0.7274], [0.7117], [0.5345] respectively.

4.6 conclusions:

- The PVA\$AgNo_3$ films have been synthesized using casting methods.
- The irradiation of the PVA\$AgNo_3$ films with x-ray doses induces color change and The color intensity was increase with increasing x-ray doses.
- X-ray Fluorescence analysis showed that the intensity of AgLα characteristic X-Ray line depends on the Ag concentration in the PVA/AgNO3 films.
- The optical densitometer analysis showed positive correlation between $AgNO_3$ concentrations and optical density of PVA/$AgNO_3$ composites films with correlation coefficient $\mathbf{R^2 = 0.9852}$ and the correlation equation **Y= 0.1622X+2.4171.**
- The optical densitometer analysis showed positive correlation between irradiated x-ray Doses and optical density of PVA/$AgNO_3$ composites films with correlation coefficient $\mathbf{R^2 = 0.8954}$ and the correlation equation **Y= 0.3834X+0.0792**.
- the synthetic PVA/Ag films can be used as chemical radiation dosimeters according to the linear relationship between x-ray doses and optical density and the sensitivity of PVA/Ag films to low x-ray doses which showed color change.

4.7 Recommendations:

The main aspects to take into consideration for future perspectives are the following:

- PVA/$AgNO_3$ composite films can be used as a chemical radiation dosimeter to measure the x-ray doses in diagnostic radiology centers in Sudan because of its good result, fast, easy and cheap assessment tool.

- We recommend using modern techniques to synthesize the PVA/$AgNO_3$films with suitable envelope.

- Radiation phantom could be developed from PVA/$AgNO_3$ materials for quality control purposes in diagnostic radiology.

- Further work is needed to know how the film thickness is affecting by the radiation dose.
- Studying temperature dependence on the fluorescence of the dosimeter would be the next step, as well as determine the right storage and measurement conditions of PVA/$AgNO_3$ films.
- Attention has been paid to evaluate a new synthesis method of silver nanoparticles in a solid-state host matrix and to investigate the influence of synthesis parameters and matrix characteristic on the distribution, shape, and size of silver nanoparticles.

4.8 References:

Abdo Mohd Meftah, Elham Gharibshahi, Nayereh Soltani, W. Mahmooud Mat Yunus and Elias Saion, Structural, Optical and Electrical Properties of PVA/PANI/Nickel Nanocomposites Synthesized by Gamma Radiolytic Method, *Polymers* 2014, *6*, 2435-2450; doi:10.3390/polym6092435.

Ali Z.I., Hossam M. Said and H.E. Ali. (2006), "Effect of electron beam irradiation on the structural properties of poly(vinyl alcohol) formulations with triphenyltetrazolium chloride dye (TTC)". Radiation Physics and Chemistry, Vol. 75 (1), Pp. 53–60.

Al-Zahrany AA, Rabaeh KA, Basfer AA (2011). Radiation induced color bleachingof methyl red in polyvinyl butyral film dosimeter. Radiat. Phys. Chem. 80:1263-1267.

A. Miller, "Dosimetry for Radiation Processing," Radiation Physics and Chemistry, Vol. 28, No. 5-6, 1986, p. 321.

Andreo, P., Burns, D.T., Nahum, A.E., Seuntjens, J., and Attix F.H. (2017). Fundamentals of Ionizing Radiation Dosimetry. WILEY-VCH.

A.N.Goldstein, C.M. Echer, and A.P. Alivisatos,the journal of Science 256 (1992) 1425-1427.

A Primer, 1996 Fundamentals of UV-visible spectroscopy, Hewlett-Packard publication number 12-5965-5123E, Germany.

Arshak, K. and Korostynska, O. (2003) Gamma Radiation-Induced Changes in the Electrical and Optical Properties of Tellurium Dioxide Thin Films. IEEE Sensors Journal, 3, 717. http://dx.doi.org/10.1109/JSEN.2003.820327.

Avenue, Dublin, Ireland, British Journal of Radiology 75 (2002),243-248 © 2002.

B. G. Steetman, S. K. Banerjee, Solid State Electronic Devices,Pearson Education Inc (2006) ISBN 0-13-149726-X.

Blaskov V, Stambolova I, Shipochka M, Vassilev S, Kaneva N, Loukanov A (2011). Decoloration of Reactive Black 5 Dye on TiO2 Hybrid films Deposited by Sol-Gel Method., Scientific papers, Vol: 38, Book 5, 2011- Chemistry.

Boone, J.M. 2000, "X-ray production, interaction and detection in diagnostic imaging" in Handbook of medical imaging Volume 1. Physics and Psychophysics, ed. Beutel J., Kundel H.L., Van Metter R.L., 1st edn, SPIE, Washington, USA, pp. 3-81.

Bunn, C.W. 1948. Crystal structure of polyvinyl alcohol. Nature 161: 929-933.

Bushberg JT, Seibert JA, Leidholdt EM, Boone JM. The essential physics of medical imaging, 2nd ed. Philadelphia, PA: Lippincott Williams & Wilkens, :145-173, 2002.

Chen YP, Liu SY, Yu HQ, Yin H, Li QR (2008). Radiation induced degradation of Methyl Orange in aqueous solutions. Chemosphere 72:532–536.

C. W. Lee, C. H. Chou, J. H. Huang, C. S. Hsu, T. P. Nguyen, j. Mater. Sci. Eng: B, 147 (2008) 307.

C.W. Mays, J.S. Vermaak, D. Kuhlmann-Wilsdorf, Surface Science12 (1968) 134-140.

D.R. Dance, S. christofides, A.D.A. Maidment, I.D. Mclean, K.H. Ng, Diagnostic Radiology Physics, A handbook for teachers and students, ISBN 978–92–131010–1, 2014.

Drobny, J.G. (2010). Radiation Technology for Polymers. CRC Press, 2nd edition.

E.B. Podgorsak, Radiation Oncology Physics: A Handbook for Teachers and Students, international atomic energy agency vienna, 2005.

EPA-402-K-07-006, Environmental Protection Agency Office of Radiation and Indoor Air, Radiation Risks and Realities: May 2006.

G. Carotenuto, L. Nicolais, Nanocomposites, Metal-Filled, in the Encyclopedia of Polymer Science and Technology, Wiley, New York (2003).

Glenn F. Knoll, Radiation Detection and Measurement, 4th Edition, ISBN: 978-0-470-13148-0, August – 2010.

G. Wang, J. Xu, H. Chen, Biosens. Bioelectro. 24 (2009) 2494.

Hall, E.J. Lessons we have learned from our children: cancer risk from diagnostic radiology. Paediatric Radiology, vol. 32, pp,2002: 700-706.

Han, D.; Yan, L.; Chen,W.; Li,W. Preparation of chitosan/graphene oxide composite film with enhanced mechanical strength in the wet state. Carbohydr. Polym. 2011, 83, 653–658.

Huda, W. 2010, *Review of radiologic physics*, Third Editon edn, Lippincott Williams & Wilkins, Philadelphia.

IAEA Radiation oncology physics: A Handbook for Teachers and Students – 16.2.1 Slide 2 (9/236) (2005).

International Committee for Radiation Protection (lCRP). Committee 3. 2001: Diagnostic Reference levels in Medical imaging.

Iskandar Shahrim Mustafa, Norhanisah Megat Azman, Azhar Abdul Rahman,
Ramzun Maizan Ramli and Halimah Mohamed Kamari, Journal of Engineering Science, Vol. 9, 61–69, 2013

Jin R, Cao Y, Mirkin C A, Kelly K L, Schatz G. C. and Zheng J. 2001. Photo induced conversion of silver nanospheres to nanoprisms. Science 294, 1901-1908.

Jiri George Drobny," Radiation Technology for Polymers", CRC Press LLC, (2003).

J.R. Weertman, D. Farkas, K. Hemker, H. Kung, M. Mayo, R. Mitra, H.V. Swygenhoven, MRS Bull. 24 (1999) 44-53.

J. Schiøtz,, K.W. Jacobsen, Science 301 (2003) 1357-1359.

Khanmohammadi H, Erfantalab M (2012). New 1, 2,4-triazole-based azo- azomethine dyes. Part I: Synthesis, characterization and spectroscopic studies. Spectrochimica Acta Part A: Mol. and Biomol. Spect. 86:39-43.
Knoll, G.F. (2010). Radiation Detection and Measurement. John Wiley & Sons, 4th edition.

Lee, H.; Mensire, R.; Cohen, R.E.; Rubner, M.F. Strategies for hydrogen bonding based layer-by-layer assembly of poly (vinyl alcohol) with weak polyacids. Macromolecules 2011, 45, 347–355.

Lin, J. C., C. Y. Wang. 1996. Effects of surfactant treatment of silver powder on the rheology of its thick-film paste. Material Chemical Physics 45: 136-144.

Li W, X Zhao, Z Huang and S Liu, Nanocellulose fibrils isolated from BHKP using ultrasonication and their reinforcing properties in transparent poly (vinyl alcohol) films *Polym Res* 20 210 (2013).

L. Liu, H. Song, L. Fan, F. Wang, R. Qin, B. Dong, H. Zhao, X. Ren, G. Pan, X. Bai, Q. Dai, j.Mater. Res. Bull. 44 (2009) 1385.
Lokhovitsky, V.I. and V.V. Polikarpov. 1980. Technology of radiation emulsion polymerization. Atomizdat, Moscow-Russia.

M.C. Roco, Journal of Nanoparticle Research 3 (2001) 511.

M.C. Roco,, Journal of Nanoparticle Research 4 (2002) 19.

M. G. Lines, J. Alloys. Comp. 449 (2008) 242.

M. Kattan, Y. Daher and H. Alkassiri, "A High-Dose Do- simeter-Based Polyvinyl Chloride Dyed with Malachite Green," Radiation Physics and Chemistry, Vol. 76, No. 7, 1989, pp. 1195-1199. doi:10.1016/j.radphyschem.2006.12.004.

Mohammed A. Ali Omer, Hamed A. Ismail, Mohamed E. M. Garlnabi, Ghada A. Edam, Nuha S. Mustafa, Optimization of PAV\AgNO3 Films for Measuring Entrance and Exit Radiotherapy Dose Relative to TLDs, International Journal of Science and Research (IJSR), Volume 4 Issue 3, March 2015

Molyneux., 1983. Water Soluble Synthetics Polymers: Properties and Behavior. Vol.1. CRC. Press. USA.

Muhammad Attique Khan Shahid1, Bushra Bashir, Hina Bashir, Huma Bashir1 and Arfa Mubashir, Dosimetric characterization and spectroscopic study of radiochromic films as natural dye dosimeters, International Journal of Chemistry and Material Science Vol. 2(2), pp. 028-045, June, 2014.

Murat Beyzadeoglu • Gokhan Ozyigit • Cuneyt Ebruli Basic Radiation Oncology ISBN: 978-3-642-11665-0 e-ISBN: 978-3-642-11666-7, 2010.

Mutsuo, S.; Yamamoto, K.; Furuzono, T.; Kimura, T.; Ono, T.; Kishida, A. Release behavior from hydrogen-bonded polymer gels prepared by pressurization. J. Appl. Polym. Sci. 2011, 119, 2725–2729.

M. Zhao, J.C. Li, Q. Jiang, J. Alloys. Comp. 361 (2003) 160-164.

N. V. Bhat, M. M. Nate, R. M. Bhat and B. C. Bhatt, "Effect of Gamma Radiation on PVA Films Doped with Some Dyes and Their Use in Dosimetric Studies," Indian Journal of Pure & Applied physics, Vol. 45, No. 6, 2007, pp. 545-548.

Nagaraja, N., Subba Reddy, C.V. Sharma, A. K. Narasimha Rao, V. V. R. 2002. DC conduction mechanism in polyvinyl alcohol film doped with potassium thiocyanate. Journal of power source 112: 326-330.

National Radiological Protection Board: Doses to Patients from Medical X-ray Examinations in the UK. 2000, NRPB.

National Radiological Protection Board: National Protocol for Patient Dose measurement in diagnostic Radiology, Dosimetry Working Party of the institute of physical Science in Medicine in, UK. 1992, NRPB.

Omer M. A. A. Saion E. Gar-elnabiM. E. M., Balla E. A. A. Dahlan Kh. M. Yousif Y. M. (2011), Gamma Radiation Synthesis and Characterization of Polyvinyl Alcohol/ Silver Nano Composites Film, J.Sc. Tech 12. (1) 2011.

Parwate DV, Sarma ID, Batra RJ (2007). Preliminary feasibility study of congo red dye as a secondary dosimeter. Rad. Meas. 42(9):1527-1529.

Patel HM, Dixit BC (2012). Synthesis, characterization and dyeing assessment of novel acid azo dyes and mordent acid azo dyes based on 2-hydroxy-4- methoxybenzophenone-5-sulfonic acid on wool and silk fabrics. Int. J. Saudi Chem. Soc. In press.

P. Buffat, J.-P. Borel, Physical Review A 13 (1976) 2287-2298.

P. MAYLES, A. NAHUM, JC. ROSENWALD, (2007) Hand Book of Radiotherapy Physics Theory and Practice, ISBN-13:978-0-7503-1, ISBN-10:0-7503-0860-5.

Ronald Denderehand, X-ray absorptiometry for measurement of bone mineral density on a slot-scanning X-ray imaging system (2014).

S.A. Baeurle (2009). "Multiscale modeling of polymer materials using field-theoretic methodologies: a survey about recent developments". Journal of Mathematical Chemistry 46 (2): 363–426. doi:10.1007/s10910-008-9467-3.

Saphwan Al-Assaf, Xavier Coqueret, Khairul Zaman Haji Mohd Dahlan, Murat Sen, Piotr Ulanski, The Radiation Chemistry of Polysaccharides, International Atomic Energy Agency Vienna, 2016, Identifiers: IAEAL 16-01075 | ISBN 978–92–0–101516–7.

Shaheen Akhtar, Taqmeem Hussain, Aamir Shahzad, Qamar-ul-Islam, Muhammad Yousuf Hussain and Nasim Akhtar, Radiation Induced Decoloration of Reactive Dye in PVA Films for Film Dosimetry, Journal of Basic & Applied Sciences, 2013, 9, 416 419.

Shuai, C.; Mao, Z.; Lu, H.; Nie, Y.; Hu, H.; Peng, S. Fabrication of porous polyvinyl alcohol scaffold for bone tissue engineering via selective laser sintering. Biofabrication 2013, 5, 015014.

Stakheev A.Y., Kustov L.M. (1999). Effects of the support on the morphology and electronic properties of supported metal clusters; modern concepts and progress in 1990s. Applied Catalysts, A188: 3-7.

Susilawati and Aris Doyan, Dose Response and Optical Properties of Dyed Poly Vinyl Alcohol-Trichloroacetic Acid Polymeric Blends Irradiated with Gamma-Rays, American Journal of Applied Sciences 6 (12): 2071-2077, ISSN 1546-9239 (2009).

Thayalan, basic radiological physics: New Delhi; jaypee brothers first edition ISBN 13: 9788171798544 :(2001).

Vadapalli Chandrasekhar," Inorganic and Organometallic Polymers", Springer-Verlag Berlin Heidelberg, P. 1, 78, 80 (2005).

V. M. Harik, M. D. Salas, Trends in Nanoscale Mechanics, Kluwer Academic Publishers (2003).

V. Singh, P. Chauhan, J. Phy. Chem. Solid. 70 (2009) 1074.

V. Yamakov, D, Wolf, S.R. Philipot, A.K. Mukherjee, H. Gleiter, Philos.j. Mag. Lette. 83 (2003) 385-393.

W. A. Jabbar, N. F. Habubi, S. S. Chiad, Optical Characterization of Silver Doped Poly (Vinyl Alcohol) Films, Journal of the Arkansas Academy of Science, vol: 64, 2010.

Wang, Y., N. Toshima 1997. Preparation of Pd-Pt Bimetallic Colloids with Controllable Core/Shell Structures. J. Phys. Chem. B 101: 5301-5306.

William R. Hendee, Ph.D. E. Russell Ritenour, Ph.D. (2002), MEDICAL IMAGING PHYSICS, ISBN 0-471-38226-4, New York, NY 10158-0012, (212) 850-6011.

W. L. McLaughlin, A. W. Boyd, K. H. Chadwick, J. C. McDonald and A. Miller, "Dosimetry for Radiation Proc-essing," Taylor & Francis, New York, 1989.

Wolfgang Demtroder, Atoms, Molecules and Photons An Introduction to Atomic, Molecular and Quantum Physics, ISBN-10 3-540-20631-0ISBN-13 978-3-540-20631-6Springer Berlin Heidelberg New York, 2006.

Yano, S., Kurita K., Lwata K., Furukawa T., Kodomari M. 2003. Structure and properties of poly(vinyl alcohol)/tungsten trioxide hybrids. Polymer 44: 3515-3522.

Yoshio Waseda, Eiichiro Matsubara, Kozo Shinoda 2011 X-Ray Diffraction Crystallography, Introduction, Examples and Solved Problems, ISBN 978-3-642-16634-1 e-ISBN 978-3-642-16635-8, DOI 10.1007/978-3-642-16635-8 Springer Heidelberg Dordrecht London New York

Zoetelief, J,. M. Fitzgerald, W. Leitz et al.1996: European protocol on dosimetry in mammography. EUR 16263 EN.